

## SPUTTER DEPOSITION FOR VLSI

*Sputtering* is a term used to describe the mechanism in which atoms are dislodged from the surface of a material by collision with high energy particles. It has become the most widely utilized deposition technique for a variety of metallic films in VLSI fabrication, including aluminum, aluminum alloys, platinum, gold, titanium:tungsten and tungsten. It is also used in some applications to deposit molybdenum, Si, SiO<sub>2</sub> (silica glass), and refractory metal silicides, although CVD or evaporation may be more frequently used to deposit this group of materials.

Sputtering has displaced evaporation as the workhorse PVD method for VLSI because of the following advantages:

- Sputtering can be accomplished from large-area targets, which simplifies the problem of depositing films with uniform thickness over large wafers;
- Film thickness control is relatively easily achieved by selecting a constant set of operating conditions and then adjusting the deposition time to reach it;
- The alloy composition of sputter-deposited films can be more tightly (and easily) controlled than that of evaporated films;
- Many important film properties, such as step coverage and grain structure, can be controlled by varying the negative bias and heat applied to the substrates. Other film properties, including stress and adhesion, can be controlled by altering other process conditions, such as power and pressure;
- The surface of the substrates can be sputter-cleaned in vacuum prior to initiating film deposition (and the surface is not exposed again to ambient after such cleaning);
- There is sufficient material in most sputter targets to allow many deposition runs before target replacement is necessary, and;
- Device damage from x-rays generated during electron-beam evaporation is eliminated (although some other radiation damage may still occur).

As is true with other processes, however, sputtering also has its drawbacks. They are:

- Sputtering processes involve high capital equipment costs;
- The deposition rates of some materials are quite slow (e.g. SiO<sub>2</sub>);
- Some materials (e.g. organic solids) are frequently unable to tolerate ionic bombardment, and degrade in a sputter environment; and,
- Since the process is carried out in low-medium vacuum ranges (compared to the high vacuum conditions under which evaporation is conducted), there is greater possibility of incorporating impurities into the deposited film.

In general, the sputtering process consists of four steps: 1) ions are generated and directed at a target; 2) the ions sputter target atoms; 3) the ejected (sputtered) atoms are transported to the substrate, where; 4) they condense and form a thin film. Although it is of interest to note that sputtering can be conducted by generating the energetic incident ions by other means (e.g. ion beams), in virtually all VLSI sputtering processes their source is a glow-discharge. The discussion of sputtering in this section will be limited to *glow-discharge sputtering*<sup>4,5,12</sup>.

### Properties of Glow Discharges

The energetic particles used to strike target materials to be sputtered in VLSI sputter deposition systems are generated by glow-discharges<sup>4,5</sup>. A *glow-discharge* is a self-sustaining

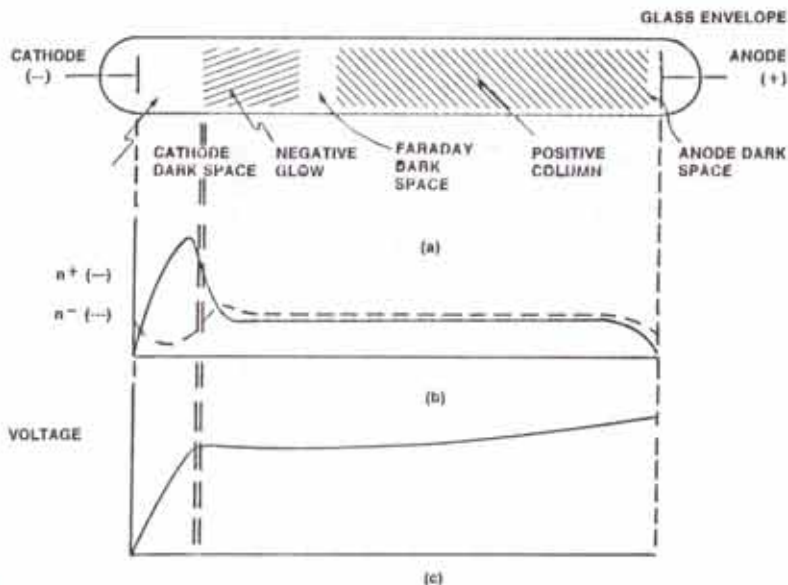


Fig. 3 (a) Structure of a glow discharge in a dc diode system. (b) Charged particle concentration in a glow discharge. (c) Voltage variation in a dc diode glow discharge. Courtesy of MRC.

type of plasma (i.e. a *plasma* is defined as a partially ionized gas containing an equal number of positive and negative charges, as well as some other number of non-ionized gas particles). In Fig. 3 we show a simple *dc diode type* system that can be employed to study the properties of glow-discharges used in sputtering. It consists of a glass tube which is evacuated and then filled with a gas at low pressures. Within the tube there are two electrodes (a positively charged *anode* and a negatively charged *cathode*) between which a dc potential difference is applied.

### Creation of Glow Discharges

Let us consider this system to examine the situation when the tube is filled with argon at an initial pressure of 133 Pa (1 torr), the distance between the electrodes is 15 cm, and a 1.5 kV potential difference is applied between the cathode and anode. At the outset no current flows in the circuit, as all the argon gas molecules are neutral and there are no charged particles in the gas. The full 1.5 kV is thus dropped between the electrodes. If a free electron is introduced into the tube (most likely created from the ionization of an argon atom by a passing cosmic ray), it will be accelerated by the electric field existing between the electrodes (whose magnitude is:  $E = V/d = 1.5 \text{ kV} / 15 \text{ cm} = 100 \text{ V/cm}$ ).

The average distance that a free electron will travel in an Ar gas at 133 Pa before colliding with an Ar atom (i.e. the mean free path), is 0.0122 cm (see Chap. 3). Most electron-atom collisions are *elastic*, in which virtually no energy is transferred between the electron and gas atom (because of the very light mass of the electron compared to a gas atom). Thus, the mean distance traveled by an electron before it makes an *inelastic* collision (in which significant energy is transferred to the atom, by the excitation of an atomic electron to a higher energy level in the atom, or to escape from the atom) is about ten times the mean free path, or 0.122 cm. If this is the *mean distance traveled by electrons between inelastic collisions*, there must be a significant

number of electron path lengths between inelastic collisions in the range of 0.5-1.0 cm. If a free electron travels 1 cm in the 100 V/cm electric field, it will have picked up 100 eV of kinetic energy. This is sufficiently high so that during an inelastic collision, enough energy can be transferred to the orbital electrons of the Ar atoms to cause their excitation or ionization. If the transferred energy,  $E$ , is less than the ionization potential (e.g. 11.5 eV  $< E < 15.7$  eV for Ar), the orbital electron will be excited to a higher energy state for about  $10^{-8}$  sec, and then return to the ground state with the emission of visible-light photons. Such excitation is the source of light emission in glow-discharges.

If the energy transferred is greater than the ionization potential (i.e.  $>15.7$  eV for Ar), a second free electron (and positive ion) will be created. Subsequently, both free electrons will become accelerated again, and the opportunity for cascading the number of free electrons and creating a condition known as *gas breakdown* exists. Figure 4 shows the breakdown voltage required to initiate discharge, as function of the product of the pressure,  $P$ , and the electrode spacing,  $d$ . When the condition of gas breakdown is reached, current flows in the external circuit as the collision-generated free electrons are collected by the anode. Each new ionization event, however, will take place closer to the positively charged anode (as the electrons are accelerated in its direction). Therefore, the current will increase to a maximum and quickly decay to zero, unless there is a mechanism available for generating additional free electrons for sustaining the current flow. When a sufficient number of electrons are available to maintain the discharge, the discharge is said to be *self-sustained*. The source of such electrons is discussed later.

#### Structure of Self-Sustaining Glow Discharges and Their Dark Spaces

A self-sustaining discharge in a system (as shown in Fig. 3) exhibits certain characteristics. First, at equilibrium the voltage drop between the electrodes is reduced (e.g. in our example, from 1.5 kV to about 150 V), and the discharge current builds up to the point that the voltage drop across the current limiting resistor is equal to the difference between the supply voltage and the electrode potential difference. Second, the discharge has a particular structure, as shown in Fig. 3a. The most important region of the discharge is the *Crookes dark space* between the negative glow and the cathode. In Fig. 6b, we see that the positive ions of the discharge are present in higher density in front of the negatively charged cathode, producing a localized *space charge* there. Any electrons near the cathode are rapidly accelerated *away* from it, due to their relatively light

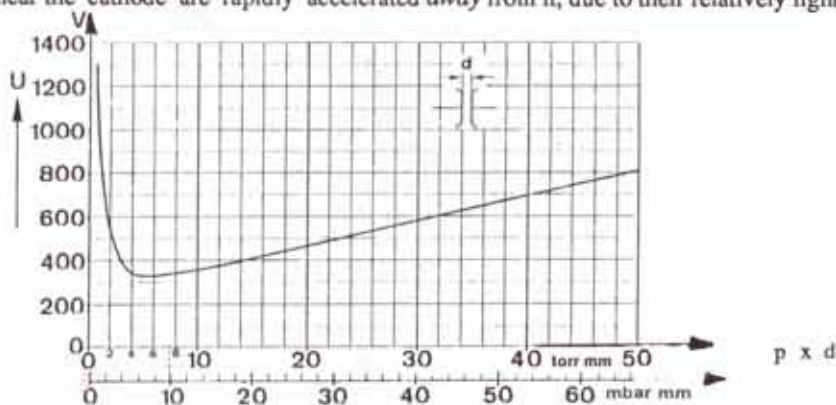


Fig. 4 Breakdown voltage,  $U$ , between two parallel plane electrodes in a homogeneous electric field as a function of gas pressure,  $p$ , and electrode distance,  $d$ , for air (Paschen curve).

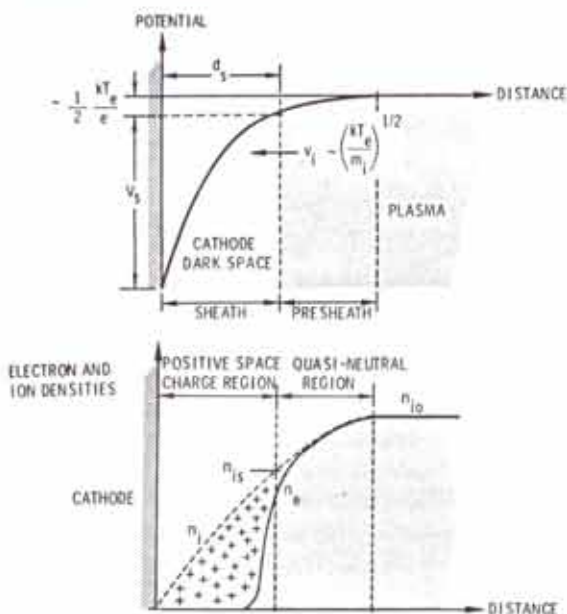


Fig. 5 Schematic representation of the positive space charge region that develops over a cathode<sup>13</sup>. Reprinted with permission of Academic Press.

mass. The much more massive ions are accelerated *toward* the cathode, but much less quickly. Thus, on average, they spend more time than electrons traversing the Crookes dark space, and at any instant their concentration in the dark space is greater than that of electrons.

This has the net effect of greatly increasing the electric field immediately in front of the cathode, and also of screening the remainder of the discharge from the cathode voltage. As a result, the electric field in the rest of the discharge is rather low and uniform, and the glow regions of the discharge are therefore more truly plasma-like (as defined at the outset of this section), than the dark space regions, which do not contain equal concentrations of positive and negatively charged particles. The greatest part of the voltage between the anode and cathode is thus dropped across the Crookes dark space, and therefore charged particles (ions and electrons) experience their largest acceleration in this region.

The reduced luminosity of the dark space is also due to the electric field present across the dark space. That is, since electrons in the dark space are strongly accelerated and traverse through the space quickly, the electron density at any instant in the dark space is drastically reduced (Fig. 5). Although there are fewer electrons, those present can gain high energies from acceleration by the electric field. When they collide with gas atoms in the dark space, they are thus more likely to cause *ionization*, rather than *excitation* events. As a result fewer light-generating electron-atom collisions occur than in the negative and positive glow regions.

When positive ions from the negative glow region enter the Crookes dark-space, they experience the strong local electric field and become accelerated toward the cathode. They also have a high probability of exchanging their charge with neutral atoms in the dark space. In doing so, they retain their momentum, while losing their charge. The formerly neutral recipient atom becomes an ion, and only at that time can begin accelerating towards the cathode. The effect of

this *charge transfer mechanism* was studied by Davis and Vanderslice, and a summary of their results is shown in Fig. 6. The data concludes that *virtually no ions reach the target with the full dark space energy*. In addition, it implies that the *cathode is bombarded by energetic neutral atoms as well as energetic ions*, and thus both species apparently produce sputtering events.

The source of electrons that sustains the discharge is the cathode, which emits secondary electrons when struck by ions. (The mechanisms of such emission are discussed in more detail in a subsequent section.) Thus, upon entering the dark space from the cathode, the electrons are accelerated by the dark space field toward the anode. Upon colliding with atoms in the dark space, they cause ionization, and are also slowed. As slower electrons, they are less energetic and thus the probability of colliding with Ar atoms and causing excitation rather than ionization events is increased. The edge of the negative glow region therefore provides an indication of where such slowed electrons start to be created in large numbers (as a result of high energy, inelastic collisions). If the pressure in the tube is reduced, the distance that the emitted electrons travel before colliding and becoming slowed, becomes longer. Consequently, the dark space lengthens. If the pressure becomes too low, the dark space extends the full length between the electrodes, and the glow-discharge extinguishes. For dc diode sputtering systems, this effect limits the minimum practical pressure for sputter deposition to the range of 10-40 mtorr (1.3-5.2 Pa). The long dark spaces of dc diodes are also an indication that the electrons are not efficiently utilized to produce ions. Thus, we shall see later how magnetic fields are employed to increase the electron path length in the course of traversing the region between cathode to anode [magnetron sputtering]. This increases the probability that the electrons undergo an ionizing collision before being collected by the anode. The dark space in such magnetron sputtering systems is typically reduced from 1-2 cm to ~0.5 mm.

#### Obstructed Glow Discharges and Dark-Space Shielding

In dc diode configurations, there must be sufficient electrons emitted at the cathode to keep the discharge self-sustaining, and these electrons must undergo an adequate number of

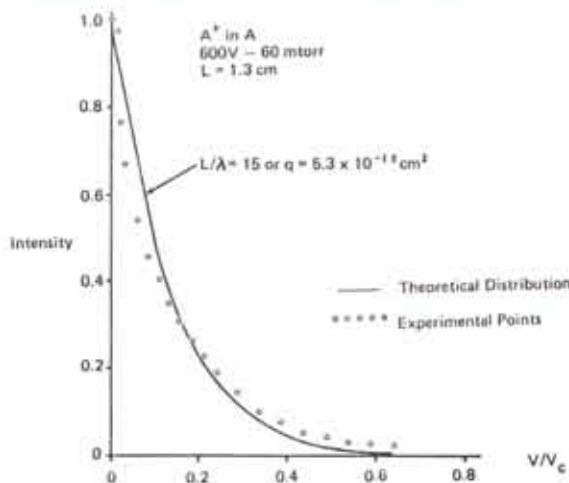


Fig. 6 Energy distribution for  $\text{Ar}^+$  from an argon discharge<sup>7</sup>. Reprinted with permission of the American Physical Society.

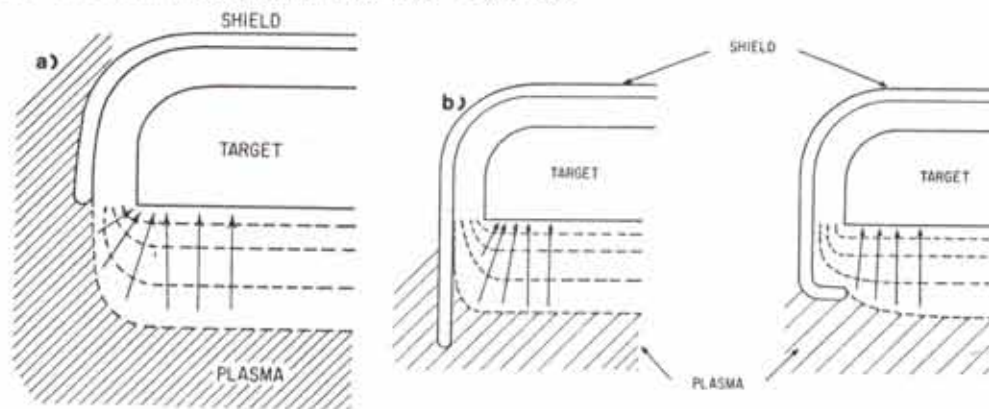


Fig. 7 (a) Potential distribution in vicinity of cathode shield (b) Reducing rim effect by extending cathode shield. (c) Reducing rim effect by wrapping shield around the cathode<sup>15</sup>. From L. Maissel and R. Glang, Eds., *Handbook of Thin Film Technology*, 1970. Reprinted with permission of McGraw-Hill Book Company.

ion-producing collisions with the sputter gas. These electrons are produced by ion bombardment of the cathode. Thus, there only needs to be a sufficient number of ions produced in the dark space (and in the glow regions) to produce enough secondary electrons to sustain the glow-discharge. As a result, as long as enough ions are produced in the dark space and glow regions, the exact location of the anode is not important. In fact, if the anode is gradually moved closer to the cathode, the positive column shown in Fig. 3 first disappears, then the Faraday dark space vanishes. Finally, a substantial fraction of the negative glow may be extinguished, before any significant effect on the electrical characteristics is observed. If the anode gets too close to the dark space, the ion production rate becomes reduced, and the voltage across the electrodes must rise to increase the secondary electron emission. Such a glow is known as an *obstructed glow*. In most practical sputter deposition systems the glow is obstructed. That is, in order to most effectively collect the sputtered material onto the substrate, the anode (on which the wafers are sometimes mounted) is placed as close to the cathode as possible (typically just far enough away to avoid extinguishing the negative glow).

On the other hand, it is typically necessary to insure that sputtering is allowed to occur only at the front side of the target, as the back side contains cooling coils, attachment fixtures, etc., which are definitely not to be sputtered. To guarantee that no sputtering takes place except from desired surfaces, a shield of metal (at a potential equal to that of the anode) is placed at a distance less than the Crookes dark space at all other cathode surfaces (Fig. 7). Since no discharge will take place between two electrode surfaces separated by less than this distance, such shielding (termed *dark-space shielding*) is effective in preventing sputtering from unwanted cathode surfaces.

### Physics of Sputtering

When a solid surface is bombarded by atoms, ions, or molecules, many phenomena can occur. The kinetic energy of the impinging particles largely dictates which events are most likely to take place. For low energies (<10 eV), most interactions occur only at the surface of the target material. At very low energies (<5 eV) such events are likely to be limited to

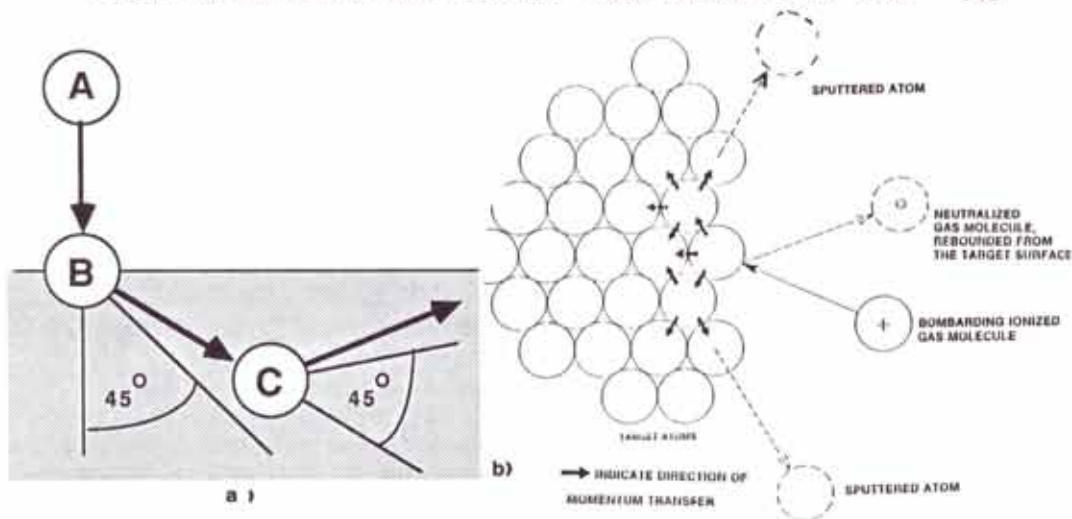


Fig. 8 (a) Binary collision between atom A and B, followed by a binary collision between atom B and C. (b) Collision process responsible for sputtering and fast neutral generation.

reflection or physisorption of the bombarding species. For low energies which exceed the binding energy of the target material (5-10 eV), surface migration and surface damage effects can take place. At much higher energies (>10 keV), the impinging particles are most likely to be embedded in the target, and this mechanism is the basis of ion-implantation. At energies between the two extremes, two other effects also arise: 1) some fraction of the energy of the impinging ions is transferred to the solid in the form of heat, and lattice damage; and 2) another fraction of such energy causes atoms from the surface to be dislodged and ejected into the gas phase (*Sputtering*).

#### Billiard Ball Model of Sputtering

The exact mechanisms which lead to the ejection of atoms under ion bombardment are not known, and a comprehensive theory of sputtering is not likely to be developed in the near future since many parameters are involved, including the kinetic energy of the ions, lattice structure, and binding energy of lattice atoms. Some of the details, however, are reasonably well understood and can be aptly described with a relatively simple momentum-transfer model. G.K. Wehner, whose theoretical work first established a solid scientific basis for sputtering, often described sputtering as a game of three-dimensional billiards, played with atoms<sup>7</sup>. Using this analogy, it is possible to visualize how atoms may be ejected from a surface as the result of two binary collisions (Fig. 8b & c) when a surface is struck by a particle with a velocity normal to the surface (e.g. atom A in Fig. 8b). Note that a *binary collision* is one in which the primary particle strikes a single object (e.g. atom B in Fig. 8b), and gives up a significant fraction of its energy to the struck atom, while retaining the remaining fraction. As a consequence of the collision, atom B may leave the point of impact at an angle greater than  $45^\circ$ . If atom B then undergoes a secondary collision with atom C, the angle at which atom C leaves the secondary impact point may again be greater than  $45^\circ$ . Thus, it is possible that atom C can have a velocity component greater than  $90^\circ$  (and thus be directed outward from the surface). As a result, there is

a finite probability that atom C will be ejected from the surface as a result of the surface being struck by atom A.

When the directions of sputtered atoms from the surface of polycrystalline materials (and most cathode materials in sputter applications are polycrystalline) are measured for the case of *normal incidence*, it is found that the ejected atoms leave the surface in essentially a cosine distribution. A cosine distribution, however, does not describe the sort of small-angle ejections that would be expected from the simple collision processes described above. Evidently in actual sputtering events, more than two collisions are involved, and the energy delivered by impinging ions *during normal incidence* is so randomly distributed that the effect of the incident momentum vector is lost. Note that the energy range of sputtered atoms leaving the target is typically 3-10 eV, and that the bombarding species also recoil from the cathode face with some energy. Thus, the target surface is a source of sputtered atoms as well as energetic backscattered species.

For the case when the surface is bombarded by ions at an oblique angle (i.e.  $>45^\circ$ ), there is a higher probability that the primary collision between the incident ion and the surface atom will lead to a sputtering event. Furthermore, oblique incidence confines the action closer to the surface, and thus sputtering is enhanced. In cases of oblique bombardment, the incident momentum vector becomes important, and sputtered atoms are ejected strongly in the forward direction. In addition, the *sputtering yield*, defined as the number of atoms ejected per incident ion, may be as much as an order of magnitude larger than that resulting from normal incidence by bombarding ion (Fig. 9). This effect also leads to *faceting*, which is discussed in a later section.

### Sputtering Yield

The *sputtering yield* is important because it largely (but not completely) determines the rate of sputter deposition. Sputtering yield depends on a number of factors besides the direction of incidence of the ions, including: a) target material; b) mass of bombarding ions; and c) the energy of the bombarding ions. There is a minimum energy threshold for sputtering that is approximately equal to the heat of sublimation (e.g. 13.5 eV for Si). In the energy range of sputtering (10-5000 eV), the yield increases with ion energy and mass. Figure 10 shows the sputtering yields of copper as a function of energy for various noble gas ions. The sputtering yields of various materials in argon at different energies is given in Table 2<sup>14</sup>.

Several matters related to sputtering yield should also be noted. First, although the sputtering yields of various materials are different, as a group they are much closer in value to one another than, for example, the vapor pressure of comparable materials. This makes the

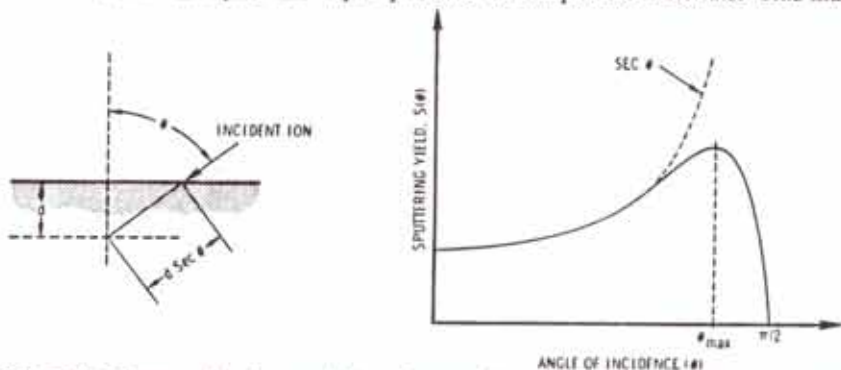


Fig. 9 Schematic diagram showing variation of sputtering yield with ion angle of incidence.



Table 2. SPUTTERING YIELDS FOR METALS IN ARGON IN ATOMS /ION

Target	At.Wt. /Dens.	100 eV	300 eV	600 eV	1000 eV	2000 eV
Al	10	0.11	0.65	1.2	1.9	2.0
Au	10.2	0.32	1.65	2.8	3.6	5.6
Cu	7.09	0.5	1.6	2.3	3.2	4.3
Ni	6.6	0.28	0.95	1.5	2.1	
Pt	9.12	0.2	0.75	1.6		
Si	12.05	0.07	0.31	0.5	0.6	0.9
Ta	10.9	0.1	0.4	0.6	0.9	
Ti	10.62	0.08	0.33	0.41	0.7	
W	14.06	0.12	0.41	0.75		

deposition of multilayer films or multi-component films much more controllable by sputtering. We discuss the details of sputtering from multi-component targets in the section on *Process Considerations in Sputter Deposition*. Second, since the bombarding ions are by no means monoenergetic in glow discharge sputtering, it is not necessarily valid to use the sputtering yield values for pure metals when alloys, compounds, or mixtures are being sputtered. The tabulations of sputter yields, however, are useful for obtaining rough indications of deposition or etch rates of various materials.

#### Selection Criteria for Process Conditions and Sputter Gas

The information gleaned from sputtering yields and the physics of sputtering can also be usefully applied toward an understanding of how process conditions and materials are selected for sputtering including: a) type of sputtering gas; b) pressure range of operation; and c) electrical conditions for the glow discharge<sup>4,15</sup>. That is, in pure physical (as opposed to reactive

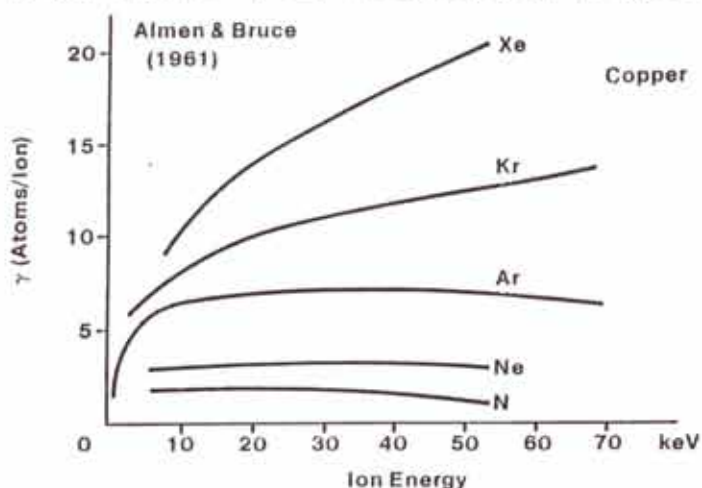


Fig. 10 Sputtering yields of the noble gases on copper, as a function of energy<sup>55</sup>.

sputtering) it is important that the ions or atoms of the sputtering gas not react with the growing film. This limits the selection of sputtering species to the noble gases. Furthermore, argon is virtually the unanimous choice, since it is easily available, is less costly than xenon or krypton, and still gives adequate sputtering yields. The *pressure range of operation* is set by the requirements of the glow discharge (lower limit  $\sim 2\text{-}3$  mtorr for magnetron sputtering) and the scattering of sputtered atoms by the sputtering gas (upper limit 100 mtorr). In addition, a desired goal of sputter deposition is to obtain maximum deposition rates. So *electrical conditions* are selected to give a maximum sputter yield per unit energy. That is, as energy is increased, each incremental energy addition gives a progressively smaller incremental sputtering yield increase. This occurs because higher energy ions implant themselves, and thus end up dissipating a greater proportion of their energy via non-sputtering processes. The most efficient ion energies for sputtering are typically obtained for electrode voltages of several hundred volts.

In general, the higher the current at the cathode, the higher is the deposition rate, since more ions are striking the cathode (and thus are causing more sputtering). The product of the cathode current and the electrode voltage gives the input power of the sputtering process. In magnetron sputtering, cathode current densities of  $10\text{-}100$  mA/cm<sup>2</sup> at a few hundred volts are typical.

From the foregoing discussion on the mechanism of sputtering, it is also reasonable to surmise that sputtering is a highly inefficient process. This is true, and in fact,  $\sim 70\%$  of the energy consumed during the sputtering process is dissipated as heat in the target, and  $\sim 25\%$  by emission of secondary electrons and photons by the target. The target heating can raise target temperatures to levels capable of damaging the target, associated vacuum components, or the bonding of the target and the backing electrode. Cooling of the target with water, or other suitable liquids is typically used to maintain low target temperatures.

### Secondary Electron Production for Sustaining the Discharge

Near the outset of the discussion on glow-discharges, it was also observed that the glow-discharge must be continuously provided with free electrons to keep it self-sustaining. In most dc sputtering systems, the source of such electrons is secondary electron emission from the target. An important mechanism for such secondary electron emission is Auger emission, although other emission mechanisms are also responsible for generating secondary electrons. The *Auger emission* process occurs according to the following sequence of events (Fig. 11): when a positive ion comes close to the target surface it appears as a potential-well of 15.67 eV to the free electrons of the target. The target electrons require a minimum of energy,  $q\Phi$ , to escape from the target (where  $\Phi$  is the work function of the target material, and  $q\Phi$  is typically 3-5 eV). Thus, some of the target electrons can tunnel into the Ar potential-well and escape the target. The energy difference between 15.67 eV and the minimum escape energy is released in the form of a photon. If this photon (e.g. of energy  $15.67\text{ eV} - 5\text{ eV} = 10.67\text{ eV}$ ), is absorbed by another target electron near the surface, this electron may then possess enough energy to be emitted from the target (i.e. the Auger electron). This sequence of events is however, rather improbable. As a result, several ion bombardment events must occur at the cathode in order for a single secondary Auger electron to be emitted. The secondary electron yield per bombarding ion,  $\gamma_1$ , has been measured to be  $\sim 0.1$  for metal targets, but is considerably higher for dielectric targets.

Besides providing a source of electrons to sustain the discharge, electron emission is also important to the sputtering process in other ways. First, ions bombarding the cathode are neutralized. Thus, it is highly probable that each ion that closely approaches the target will extract an electron from the target, and return to the discharge as a neutral atom. Second, the

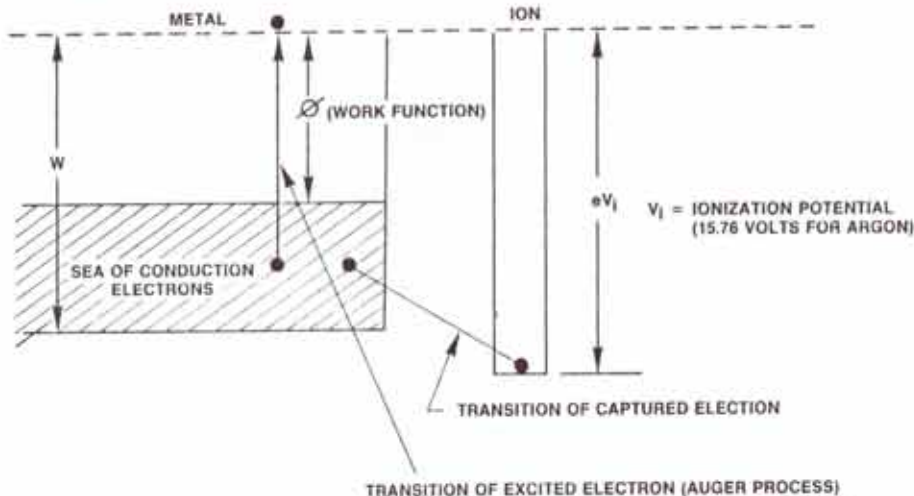


Fig. 11 Potential energy diagram for ion approaching a metal target. Courtesy of MRC.

total target current,  $I$ , is the sum of the ion flux striking the target,  $I_i$ , and the secondary electron current leaving the electrode,  $I_e$ . Since  $\gamma_i$  is larger for dielectric materials, their  $I_e$  is also larger. This implies that for the same cathode current,  $I$ , dielectrics will sputter more slowly than metals. That is, in dielectric sputtering a larger fraction of  $I$  is due to electron emission, and thus for equal values of  $I$ , a smaller ion flux is striking the dielectric target.

### Sputter Deposited Film Growth

Upon being ejected from the target surface, sputtered atoms have velocities of  $3\text{-}6 \times 10^5$  cm/sec and energies of 10-40 eV. It is desirable that as many of these sputtered atoms as possible be deposited upon the substrates and form the specified thin film. To accomplish this goal, the target and wafers are closely spaced, and target-to-wafer spacings of 5-10 cm are typical. The mean free path,  $\lambda$ , of such sputtered atoms at typical sputter pressures is less than 5-10 cm (e.g. at 5 mtorr,  $\lambda \approx 1$  cm). Thus, it is likely that the sputtered atoms will suffer collisions with the sputter gas atoms before reaching the substrate (Fig. 12). The sputtered atoms may therefore: a) arrive at the substrate with reduced energy ( $\sim 1\text{-}2$  eV); b) be backscattered to the target or the chamber walls; or c) lose enough energy so that they are thereafter transported by diffusion in the same manner as neutral sputter gas atoms. As a result of these events during the transport of sputtered atoms to the substrate, we can see how that sputtering gas pressure can alter various deposition parameters (such as deposition rate).

The formation and growth of the thin film on the substrate proceeds according to the general discussion on thin film formation given in Chap. 4. Therefore, we restrict our discussion to the events that uniquely impact the formation and growth of glow-discharge sputtered films.

The substrate surface on which we desire to deposit a film of the sputtered target material, is also subjected to impingement by many species during this process. The sputtered atoms arrive and condense onto the substrate. For a deposition rate of  $200 \text{ \AA}/\text{min}$ , a monolayer of deposited film will form approximately every second (assuming the size of a typical atom is  $\sim 3 \text{ \AA}$ ). For this case, and even for much higher deposition rates of Al (e.g.  $6200 \text{ \AA}/\text{min}$ ) the heat of

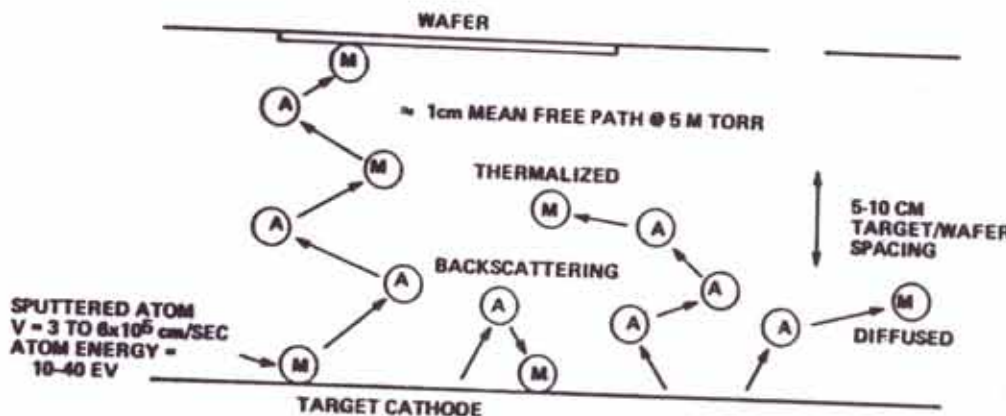


Fig. 12 Gas scattering events.

condensation is not necessarily the most important source of substrate heating.

#### Species that Strike the Substrate During Film Deposition

In addition to the sputtered atoms, the substrate is also struck by many other species (Fig. 13), the most important being: a) *fast neutral sputter gas atoms*, which retain significant energy after having struck and recoiled from the cathode. As they impinge upon the substrate, some may embed themselves in the growing film; b) *negative ions*, formed near the cathode surface by the reaction of secondary electrons and impurity gas atoms, such as O and N. These can acquire substantial energy from the Crookes dark space electric field, and thus also strike the substrate with appreciable energy; c) *high energy electrons*, which are accelerated across the Crookes dark space, and then impinge on the substrates. (In dc diode and rf diode sputtering

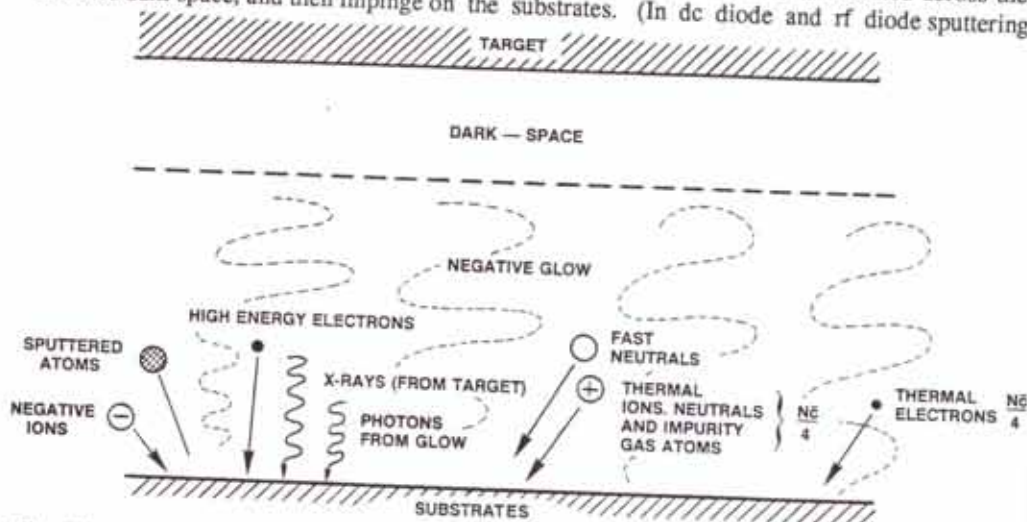


Fig. 13 Species arriving at the substrate in a sputtering system.

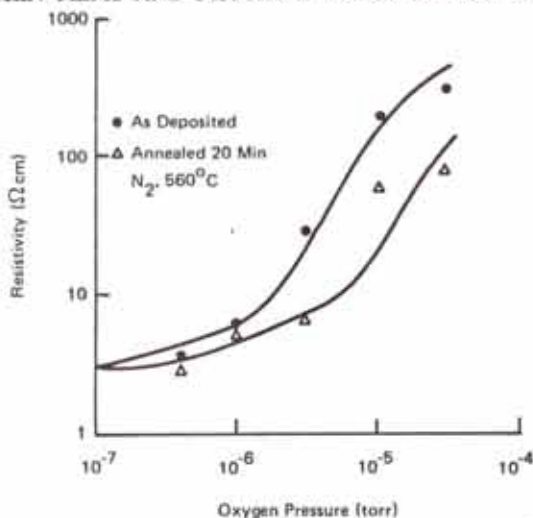


Fig. 14 Room temperature resistivity vs oxygen pressure during evaporation of 5000Å Al films at 200°C and 20 Å/s. Reprinted with permission from TRANSACTIONS OF THE METALLURGICAL SOCIETY, Vol. 242, pp. 205, a publication of the Metallurgical Society, Warrendale, Penn.

they can represent a major source of substrate heating); d) *low energy neutral sputter gas atoms* (Ar), which strike the substrate at a high flux (e.g. at 20 mtorr, the Ar flux is several thousand times greater than the arrival rate of sputtered material). However, the sticking coefficient of low energy neutral Ar atoms is considered to be negligibly small, and thus the only incorporation of Ar atoms into the growing film arises from fast neutral embedment [species (a)]; and e) *contaminants present in the form of residual gases* in the chamber can be incorporated into the growing film, particularly if they are chemically active. For example, if a sputtering system contains oxygen in the partial pressure of  $10^{-6}$  torr, the substrate surface will be struck by  $\sim 10^{15}$  oxygen atoms/sec (or 1 monolayer/sec). In Fig. 14<sup>8</sup> we observe that at  $O_2$  partial pressures of  $10^{-6}$  torr and Al deposition rates of 1,200 Å/min, the resistivity of the Al film has increased significantly due to the oxidation of some of the Al material.

The sources of residual gases can include: a) impure sputtering gas; b) outgassing from wafers/palette (or wafer holder); c) outgassing from chamber walls; and d) leaks. To minimize the presence of residual gases in sputtering, it is advisable to use highly pure sputter gases, and to continually evacuate and refill the sputter chamber to flush any residual gases being introduced through outgassing or leaks. Additional details on the effects of residual gases on sputter deposited films is given in the section on *Sputter Processing Issues*.

Up to this point in our discussion, the glow-discharge and the sputtering phenomena we have been describing, were produced by the application of a *dc voltage* between the electrodes. Sputtering performed with such systems is known as *dc glow-discharge sputtering*. The diode configuration is the simplest glow-discharge based sputtering system, and consequently it is appropriate to consider its characteristics at the outset of the discussion on sputtering. In general, however, dc diode sputtering processes possess severe limitations that render them unsuitable for most VLSI sputtering applications. As a consequence, two other glow-discharge based sputtering modes are used instead to sputter deposit thin films in semiconductor manufacture: a) radio-frequency (rf) sputtering; and b) magnetron sputtering.

## Radio-Frequency (RF) Sputtering

One of the drawbacks of dc diode systems is that they cannot be used to sputter insulators (dielectrics). As we shall explain, this is due to the fact that glow-discharges cannot be maintained with a dc voltage if the electrodes are covered with insulating layers. This represents a significant limitation, as there are several important applications which call for the sputtering of insulators, or the maintenance of a continuous discharge in the face of dielectric-covered electrodes, including: a) sputter-deposition of  $\text{SiO}_2$  films, which can be deposited as planarizing inter-metallic dielectric layers; b) the *in situ* sputter removal of thin *native-oxide* layers from silicon and aluminum surfaces prior to the deposition of overlying films (i.e. *in situ* implies that sputter etch and deposition are performed sequentially without breaking vacuum); and c) the condition of glow-discharge must be continuously maintained in some dry-etching process chambers that are equipped with electrodes coated with insulating materials.

The claim that a glow-discharge cannot be sustained if an insulator is sputtered using dc voltages is supported by the following argument: When the negatively charged cathode in dc diode systems is bombarded by ions, an electron is stripped from the cathode surface each time an impinging positive ion is neutralized. If the cathode material is a *conductor*, such electrons can be replaced by electrical conduction, and the cathode surface maintains the negative potential required to sustain the discharge. If the material is an *insulator*, the electrons lost from the cathode surface are not replaced, since electrical conduction from the insulator interior to the sputtered surface, is not possible. Therefore, the front surface accumulates a positive charge that increases with time of bombardment. This causes the potential difference (between the cathode sputter surface and the surface of the anode) to decrease (Fig. 15). As soon as it drops below the value needed to sustain the discharge, the discharge extinguishes. In practical glow-discharge configurations, the time for the insulator surface to acquire this charge is  $\sim 1\text{-}10 \mu\text{s}$  (see Prob. 5).

A technique was developed to allow replenishment of such lost electrons to the insulator surface. This involves the application of an ac voltage (rather than a dc voltage) to the electrodes, and sputtering processes based on applying this method are known as *rf sputtering*<sup>4,15</sup>. As may be expected, however, this solution introduces other complications. That is, in order to achieve a practical sputtering process by the application of ac voltages, the following conditions need to be established: a) the electrons lost from the insulator surface, by the mechanism observed in dc glow-discharge sputtering, must be periodically replenished; b) the glow-discharge must be continuously sustained under ac conditions over the full period of the ac waveform; c) an electric field configuration must be created in the process chamber which allows ions of sufficient energy to bombard and sputter the target insulator; d) sputtering in the process chamber should be

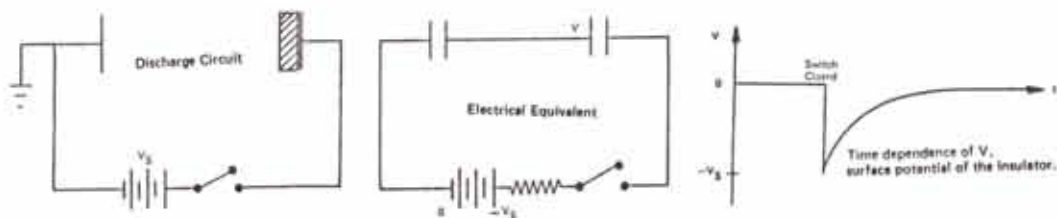


Fig. 15 Surface charging of an insulating cathode. From B. Chapman, *Glow Discharge Processes*, 1980, Copyright © John Wiley & Sons. Reprinted with permission of John Wiley & Sons.

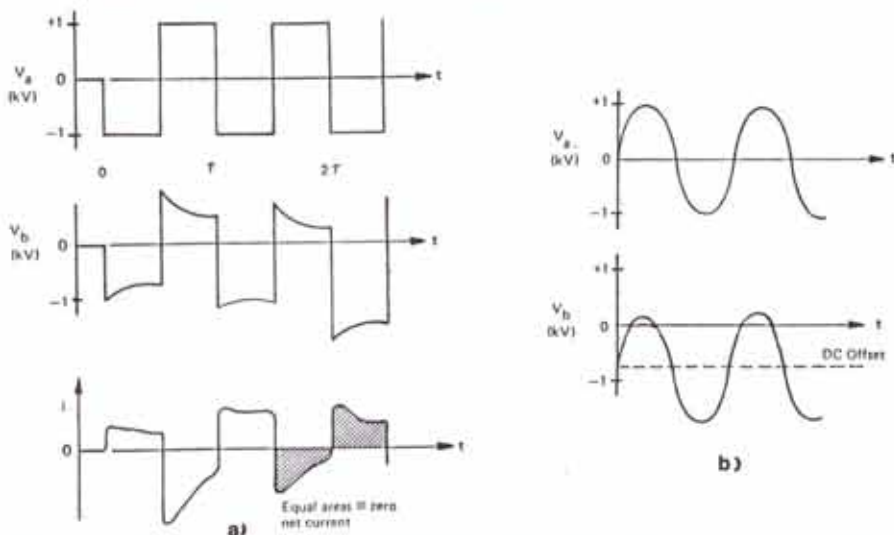


Fig. 16 (a) Voltage and target current waveforms when the circuit of Fig. 15 is square wave excited. (b) Voltage waveforms at generator ( $V_A$ ) and target ( $V_B$ ) in a conventionally sinusoidally excited rf discharge. From B. Chapman, *Glow Discharge Processes*, 1980, Copyright © John Wiley & Sons. Reprinted with permission of John Wiley & Sons.

suppressed at all surfaces except the target surface (i.e. sputtering should not occur at the chamber or non-target electrode surfaces); and e) the rf power must be efficiently coupled to the glow-discharge to maximize sputter deposition rates. We will discuss rf sputtering by explaining how each of these requirements is met. The system used to apply an ac signal to the process chamber is shown in Fig. 16. Note that we refer to the two electrodes as  $A$  and  $B$ , and no longer as cathode and anode, since the signal polarity applied to both electrodes alternates between positive and negative values.

Assume that the rf generator in Fig. 16 produces a signal of alternating polarity with an amplitude,  $V_0$ , that is large enough to cause breakdown of the process chamber gas. When such a signal is applied to the electrodes, positive ions from the discharge are accelerated toward an electrode when it is subjected to the negative-bias portion of the waveform (and electrons during the positive-bias portion). In *steady-state conditions* (to be defined), the positive charge at the target surface (e.g. electrode  $A$ ) accumulated during the negative part of the cycle, is replaced by impinging electrons during the positive part of the cycle. The net surface charge accumulated by the insulator during each complete cycle of the waveform is zero, and the lost electrons are thus replenished, and condition (a) is satisfied (Fig. 17).

As pointed out earlier, the time required to sufficiently charge the insulator surface during the negative part of the cycle to extinguish the glow-discharge is only 1-10  $\mu\text{s}$ . Therefore, low frequency ac signals to the electrodes (e.g. 60 Hz) are ineffective at maintaining a continuous glow-discharge. That is, the discharge remains ignited for only a very small fraction of the input signal period (e.g. 1-10  $\mu\text{s}$  of the 16 ms period of a 60 Hz signal). Thus, in order to satisfy condition (b) above, the charging time of insulator surfaces implies that an ac signal with a minimum frequency of 100 kHz-1 MHz must be applied to the electrodes. In practice, most ac glow-discharges are operated at 13.56 MHz (i.e. glow-discharge sputtering processes and plasma

/RIE dry etch processes). The applied power has a frequency in the radio-frequency range (hence the name *rf sputtering*), and the 13.56 MHz frequency is utilized because it is one of the frequencies designated by international communications authorities at which electromagnetic energy can be radiated without interfering with other radio-transmitted signals.

At this point it is also important to mention that rf excited discharges can be sustained without relying on the emission of secondary electrons from the target. The mechanism that allows rf excited glow-discharges to be thus sustained is not well understood, although several theories have been advanced. One theory postulates that ionization is produced by free electrons oscillating in the very weak rf field that penetrates the plasma. Such oscillations, combined with properly timed elastic collisions between the electron and gas atoms, permit the electrons to gain sufficient energy to cause ionization (despite the weak field). Two important effects are associated with this phenomenon. First, it is observed that rf excited discharges remain sustained at lower minimum pressures than dc discharges (e.g. 10 mtorr versus 40 mtorr). Second, we see that rf excitation provides a mechanism to create glow-discharges for dry etch processes without needing to be concerned about a source of electrons to sustain the discharge.

To meet condition (c) above, an electric-field in front of the target electrode must exist to accelerate the glow-discharge ions to sufficient energy to produce sputtering. Such an electric-field is produced in rf excited systems by a phenomenon known as *self-bias*. To study this phenomenon, let us examine the events that occur when the ac signal is initially applied to the insulating electrode (Fig. 16). At the time the switch is closed ( $t = 0$ ), the electrode surfaces contain no charge. The applied negative bias causes positive ions from the discharge to strike electrode A (an insulator), and to leave behind a positive charge on the surface as electrons are removed. During the positive portion of the cycle, the electrode attracts and collects electrons. The mass of the electrons is much smaller than that of ions, and the electric field accelerates them more rapidly to the electrode surface. Thus, during the two halves of the first ac cycle, many more electrons are initially collected at the electrode than ions. At the end of the first complete period, the electrode surface therefore has a net negative charge. As more cycles transpire, the negative charge continues to build up. Such negative surface charge, however, also has the

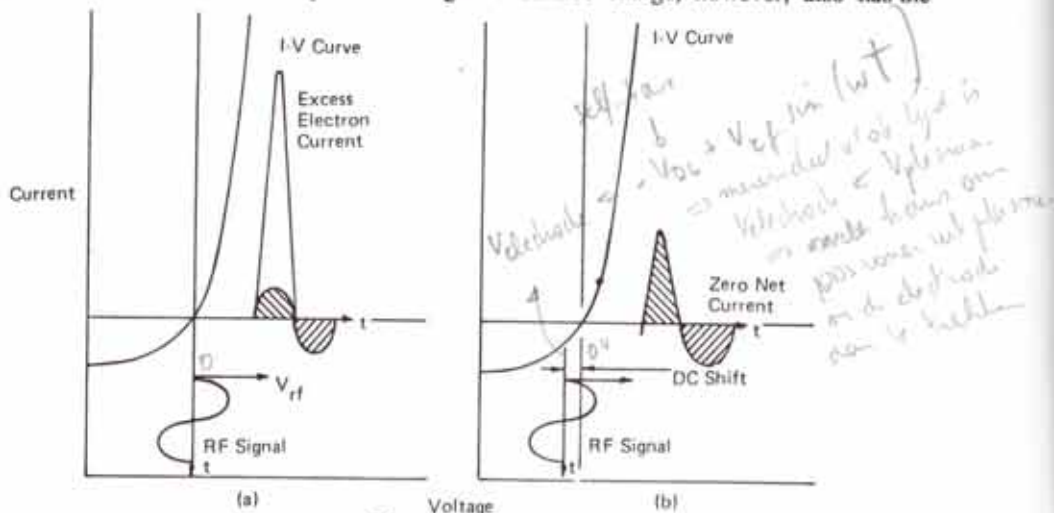


Fig. 17 Self-biasing of a dielectric surface<sup>56</sup>. Reprinted with permission of American Phys. Soc.



effect of repelling some electrons during the positive part of the cycle, and attracting positive ions more strongly during the negative parts. In the steady state, an equal number of positive ions and electrons strike the electrode during each complete signal period. The *average* charge build-up on the electrode which occurred during the first few cycles is negative, and remains constant in value under steady-state conditions. This also results in a negative dc offset voltage between the electrode and the discharge. Such a *self-bias voltage* is almost equal to the peak of the applied voltage (Fig. 16b) of the rf input signal. If the potential difference between the discharge and the self-biased electrode is sufficiently large, ions will be accelerated strongly enough toward the cathode to cause sputtering at the electrode [thus satisfying condition (c)].

Unfortunately, this effect can occur at both electrodes, as well as at any surface in the chamber connected electrically to the rf signal. To restrict the sputtering only to the target surface, the electrode configuration in the system must be altered. First, the non-sputtering electrode is grounded, and this may also be a convenient location for placing the substrate wafers onto which the sputtered film is to be deposited. Next we note that there are voltages  $V_A$  and  $V_B$  (called *sheath voltages*) occurring between the discharge and electrodes  $A$  and  $B$  respectively. To restrict sputtering only to the target (e.g. electrode  $A$ ), it is necessary for sheath voltage  $V_A$  to be large, and  $V_B$  to be as small as possible. We assume that the electrodes  $A$  and  $B$  have areas  $A_A$  and  $A_B$ , respectively.

To see how to establish such sheath voltages, we make use of an expression that describes the relationship between ion flux through the sheath, and the voltage across the sheath (Fig. 18). If a space-charge limited current is assumed, the ion current flux,  $J$ , is given by Child-Langmuir equation<sup>10</sup>:

$$J = \frac{KV^{3/2}}{\sqrt{m} D^2} \quad (1)$$

where  $V$  is the voltage drop across the sheath,  $D$  is the dark-space thickness,  $m$  is ion mass, and  $K$  is a constant. Since the current density of positive ions must be equal at both electrodes, Eq. 1 indicates that:

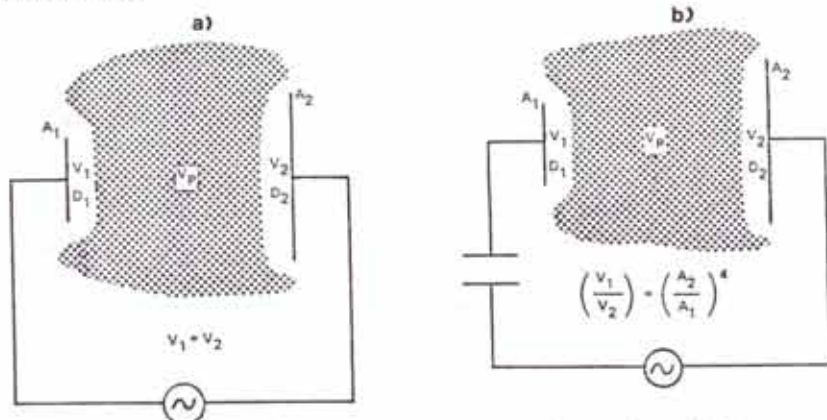


Fig. 18 (a) Voltage distribution with equal area electrodes and no blocking capacitor. (b) Voltage distribution with unequal area electrodes and blocking capacitor<sup>10</sup>. Copyright 1970 by International Business Machines Corporation; reprinted with permission.

$$\frac{V_1^{3/2}}{D_1^2} = \frac{V_2^{3/2}}{D_2^2} \quad (2)$$

Since there is a large voltage drop across the dark space, this implies that the dark space is a region of very limited conductivity. Thus, we can model the electrode-dark space-plasma as a capacitor, with capacitance proportional to electrode area and inversely proportional to  $D$ :

$$C \propto A / D \quad (3)$$

Now, an rf voltage will divide between two capacitances in series according to:

$$V_A / V_B = C_B / C_A \quad (4)$$

Using Eqs. 3 and 4, we can write:

$$V_A / V_B = (A_B / D_B) (D_A / A_A) \quad (5)$$

and substituting into Eq. 2, we get:

$$V_A / V_B = (A_B / A_A)^4 \quad (6)$$

Thus, the larger dark-space voltage will develop at the electrode having the smaller area. The fourth-power dependence is not observed in real systems (the value of the exponent is more typically determined experimentally to be  $<2$ ), but the principle of increasing the sheath voltage ratio by controlling the relative electrode areas is valid. In actual sputtering systems, the larger electrode consists of the entire sputtering chamber, including the wafer holder, which has a common electrical ground with the rf power supply. The relatively large area causes a small dark space voltage to exist, and no sputtering takes place from these surfaces. The target material is attached to the smaller electrode, which therefore develops a large dark-space voltage, and can thus experience strong sputtering. In this manner, condition (d) is satisfied.

Since the dark-space voltages  $V_A$  and  $V_B$  will not be equal if the areas of the electrodes are not equal (and the plasma is a region of equipotential), a dc voltage between the electrodes will exist. If the target is a conductor, a blocking capacitor (Fig. 19) is needed to prevent this self-bias voltage from being grounded through the rf generator. If the target was an ideal

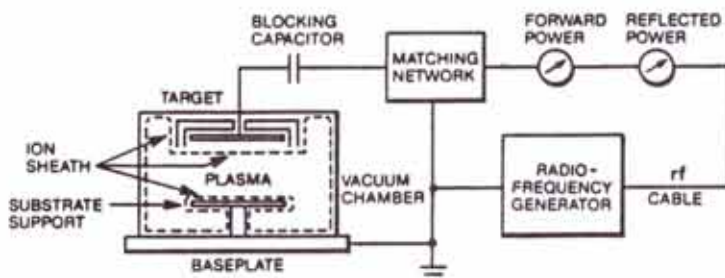


Fig. 19 Radio frequency sputtering system.

insulator, it would not be necessary to use an external *blocking capacitor*. It is common practice however, to design systems with external blocking capacitors to remove any possibility of leakage through or around the edges of the target in the presence of the plasma.

The final requirement (e), that must be satisfied in order to realize an useful rf sputter process, is to be able to couple the maximum power from the rf generator to the discharge. The output impedance  $Z_o$  of rf power supplies is designed to be purely resistive (with the value  $Z_o = 50 \Omega$ ), while the discharge has a larger and partially capacitive impedance. Therefore, an *impedance matching network* is required between the generator and discharge chamber (Fig. 19). Most systems use feedback control to tune the network to the generator by automatically maintaining minimum reflected power. This also protects the generator and coupling lines.

Rf diode sputtering systems behave in other respects much like dc diode systems. That is, secondary electrons are still emitted by the target, and subsequently accelerated through the dark space. Most still end up being collected by the grounded electrode, and thus such electrons usually represent a source of substantial substrate heating. In addition, the target is also the source of fast neutral sputter gas atoms, negative ions, and electromagnetic radiation. These species are generated in the same manner as in dc diode systems. Furthermore, rf diode configurations suffer the same inefficiency of secondary electron utilization. That is, since most electrons emitted from the target are collected by the anode, and do not cause ionization, ion production (and consequent ion bombardment of the target) is not significantly greater than in dc diode systems. Thus, for processes that require conductive materials to be deposited at high rates (e.g. aluminum or aluminum alloys), rf diode sputtering is not an optimum process.

## Magnetron Sputtering

In both dc and rf diode sputtering, most secondary electrons emitted from the target do not cause ionization events with Ar atoms. They end up being collected by the anode, substrates, etc., where they cause unwanted heating. Since most electrons pass through the discharge region without creating ions, the ionic bombardment and sputtering rate of the target (and the deposition rate on the substrates) is much lower than if more of these electrons were involved in ionizing collisions. Thus, dc diode and rf diode sputtering processes normally exhibit inadequately low deposition rates.

A technique known as *magnetron sputtering* increases the percentage of electrons that cause ionizing collisions, by utilizing magnetic fields to help confine the electrons near the target surface. By using magnetron sputtering, current densities at the target can be increased to 10-100 mA/cm<sup>2</sup>, from about 1 mA/cm<sup>2</sup> for non-magnetron configurations.

To describe the principle of magnetron configurations, first consider the motion of a charged particle of charge  $q$ , mass  $m$ , and initial velocity  $v_o$ , that is perpendicular to a uniform magnetic field,  $B$ , as shown in Fig. 20. The charged particle experiences a magnetic force,  $F = q v \times B$ , which is perpendicular to both its velocity and the direction of  $B$ . If no other forces are exerted on such a particle, it will continuously be acted upon by the force,  $F$ , and this will induce a circular motion, with radius,  $r_g$ :

$$r_g = (m v) / q B \quad (7)$$

where  $v$  is the velocity of the particle.

For electrons and Ar<sup>+</sup> ions, the equation for  $r_g$  can be expressed in terms of the energy,  $E$ , of the particles (in eV), and of the magnetic field,  $B$  (in gauss), or:

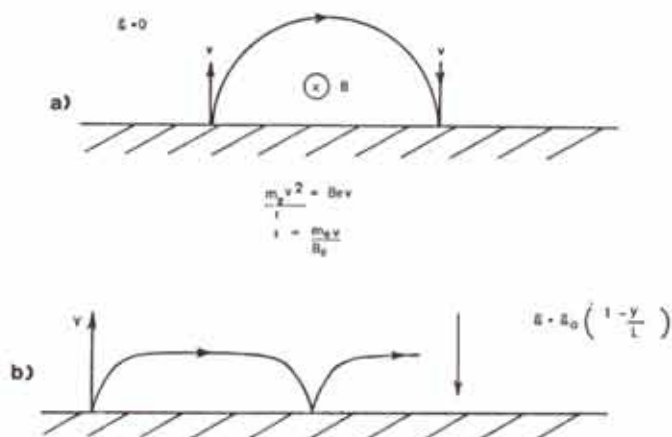


Fig. 20 (a) Motion of an electron in a region of magnetic field  $B$  parallel to the surface. (b) Motion of an electron ejected from a surface with velocity  $v$  into a region magnetic field  $B$  parallel to the surface, with no electric field and, (c) with a linearly decreasing field. From B. Chapman, *Glow Discharge Processes*, 1980, Copyright © John Wiley & Sons. Reprinted with permission of John Wiley & Sons.

$$r_g(\text{electron}) = 3.37 \times [E^{1/2}(\text{eV}) / B(\text{gauss})] \quad (8)$$

$$r_g(\text{Ar}^+) = 9.11 \times 10^2 [E^{1/2}(\text{eV}) / B(\text{gauss})] \quad (9)$$

From these equations, we can see that  $\text{Ar}^+$  ions have motion radii which are  $\sim 300$  times larger than electrons for equivalent conditions of  $B$  and particle energy. Thus, as an ion moves through the region containing the magnetic field, its  $r_g$  is so large that it essentially moves in a straight line when crossing the dark space. This illustrates that the direction of electron motion in magnetron discharges is strongly influenced by the magnetic field, while the magnetic field does not significantly change the direction of ions as they cross the dark space.

In the next case, examine the situation of an electron which is emitted from a sputtering target surface. Let there be a magnetic field,  $B$ , parallel to the surface, and an electric-field perpendicular to the surface (due to the dark space). Assume the electron is initially at rest (e.g. having just been emitted from the target), and that the magnitude of the electric-field is given by:

$$E = E_0 (1 - y/L) \quad (10)$$

where  $E_0$  is the magnitude at the surface of the target,  $L$  is the length of the dark space, and  $y$  is the vertical distance above the target. Now the electron will be initially accelerated away from the target in a direction perpendicular to the target surface by the electric field, but simultaneously it will experience a force due to the magnetic field,  $F = qv \times B$ .

The electron velocity will therefore be altered from a direction perpendicular to the surface. If the magnetic field is strong enough to deflect the electron velocity so that it begins to return to the target surface before it leaves the magnetic field, its motion will be roughly cycloidal as shown in Fig. 20c. That is, as it approaches the target surface after having been deflected, the electron will be *decelerated* by the electric field, and eventually will come to rest (momentarily) at

the target surface. At that point, the next period of the cycloid motion will be initiated, as it is once again repelled by the electric-field. The maximum excursion of the electron (with charge  $e$  and mass  $m$ ) from the target during such motion,  $y_{\max}$ , is given by:

$$y_{\max} = \frac{1}{B} \left[ \frac{2m}{e} (V - V_T) \right]^{1/2} \quad (11)$$

where  $V_T$  is the negative target voltage, and  $V$  is the potential in the dark space at  $y_{\max}$ .

The net result is that secondary electrons are trapped near the target surface by the combination of the magnetic and electric fields, and continue to move with cycloid (or *hopping*) motion until they collide with an Ar atom. Even though not every such collision produces an ionization event, many more ions are generated than if the secondary electron escaped the discharge without undergoing any collisions with Ar. The magnitude of the electron velocity *parallel* to the target surface,  $v_D$  (also known as the  $E \times B$ , or *magnetron drift velocity*), is given by:

$$v_D = \frac{10^8 E_{\perp} \text{ (V/cm)}}{|B| \text{ (gauss)}} \quad (12)$$

There are two principal magnetron electrode configuration designs used in VLSI sputtering systems: a) the *planar magnetron*; and b) the *circular magnetron*. Figure 21a shows a variety of

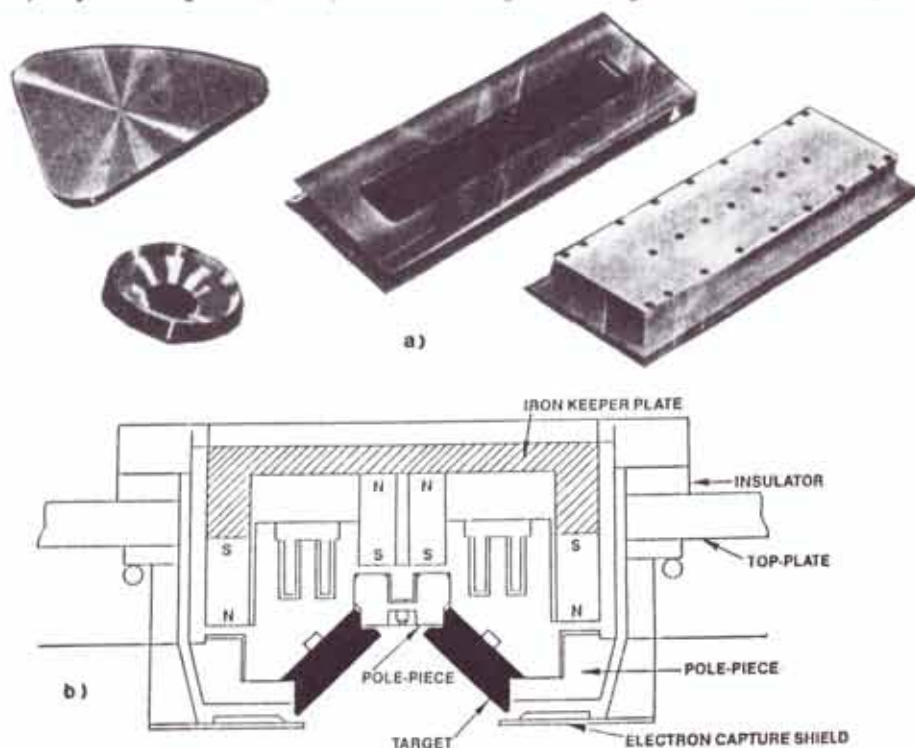


Fig. 21 (a) Sputtering targets. Reprinted with permission of Semiconductor International. (b) Focest<sup>®</sup> sputtering targets for MRC sputtering systems. Courtesy of MRC.

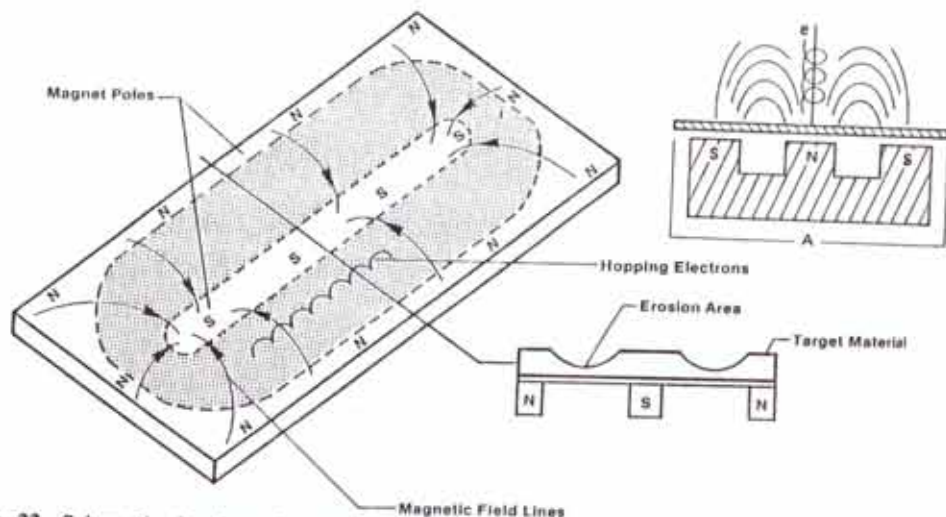


Fig. 22 Schematic drawing of planar magnetron target and magnets.

target shapes used in these systems. Note that the planar magnetron targets can be rectangular or wedge shaped. Some of such rectangular targets (e.g. MRC Focost<sup>®</sup> targets, Fig. 21b) are still thought of as planar targets, although they no longer look very planar. The shape of the planar targets are dictated by system design, although they all basically share the same principle of operation. Therefore, we limit our discussion to the rectangular planar magnetron for purposes of describing the characteristics of all planar magnetrons.

In *planar magnetrons*, the target surface is planar, and the  $\mathbf{B}$ -field is created by magnets behind the target<sup>4,5,12,39</sup>. The anode is usually a rod placed along side the cathode. (Apparently the location of the anode relative to the cathode is not critical to effective operation.) During deposition the substrates pass in front of the target. A planar-magnetron target is shown in Fig. 22a, and its cross-section, cut along A-A, to show the magnets and magnetic-field orientation, in Fig. 22b. In examining these illustrations, three things should be noted: a) half-way between the magnet poles, the magnetic field lies parallel to the target face. This is the region where the magnetron drift velocity,  $v_D$  occurs; b) the  $\mathbf{E} \times \mathbf{B}$  field that formed in this region closes on itself. Thus, a continuous path that the "hopping" electrons can traverse is established; and c) the plasma density is greatest where  $\mathbf{E} \times \mathbf{B}$  is maximized. This region is called the *race-track* and sputtering is very rapid in the race-track portion of the target. Since the race-track path is continuous, and rectangular planar magnetron targets are normally long and narrow, they form a *two-line sputter deposition source* for wafers that pass in front of the target during deposition.

Figure 22a also shows the hopping motion of the electrons as it follows the race track. Near the center of the track the maximum excursion,  $y_{max}$ , is  $\sim 0.5$  cm. The dark-space is also significantly reduced (to about 0.5 mm). Since magnetrons are much more effective in causing secondary electrons to undergo ionization collisions, much higher target currents occur for comparable voltage levels. Thus, magnetron devices have impedances of  $\sim 50 \Omega$ , as opposed to  $40,000 \Omega$  for dc diode devices. Planar magnetron devices can be operated with either dc or rf power supplies.

The particular configuration of *circular magnetrons* used in VLSI sputters systems was

invented by Clarke<sup>13</sup>, and are known as the Sputter Gun<sup>®</sup> (registered trademark of Sloan Associates), and the S-Gun<sup>®</sup> (registered trademark of Varian Associates). Figure 23a shows an example of the target shape used in such magnetrons, and Fig. 23b shows a cross-section of an S-Gun. As in other magnetrons, an intense plasma region is formed near the cathode, due to the  $E \times B$  field orientation (Fig. 23b). The anode is concentrically located, and the magnetic field is generated by annular permanent magnets as shown in Fig. 23a. In modern high-rate circular magnetron systems, the substrates are placed close to the cathode (Fig. 23d), and only a single wafer is deposited at a time. This maximizes deposition rates and efficiently collects a large percentage of the sputtered species. Figure 23d also qualitatively illustrates the flux of the sputtered species that are produced in such a circular magnetron. Note that in early systems which used circular magnetrons, the substrates were mounted on a planetary or other movable support system, as discussed in the *Evaporation* section. This also provided an inexpensive vehicle for implementing a sputtering capability, because existing evaporation systems could be retrofitted with an S-Gun.

The hopping motion along the target surface that constrains electrons to the region near the cathode surface of the circular magnetron is shown in Fig. 23b. The target erodes as material is sputtered away as shown in Fig. 23c. Efforts to maintain satisfactory film thickness uniformity across large diameter wafers together with a higher percentage of material utilization from the target, have led to such modifications in circular target designs as: a) multiple concentric cathodes; and b) non-planar target cathode surfaces.

### Bias Sputtering

The surfaces of the substrates during glow-discharge sputtering always acquire a negative potential, albeit usually small, with respect to the plasma. Thus, they are subject to some

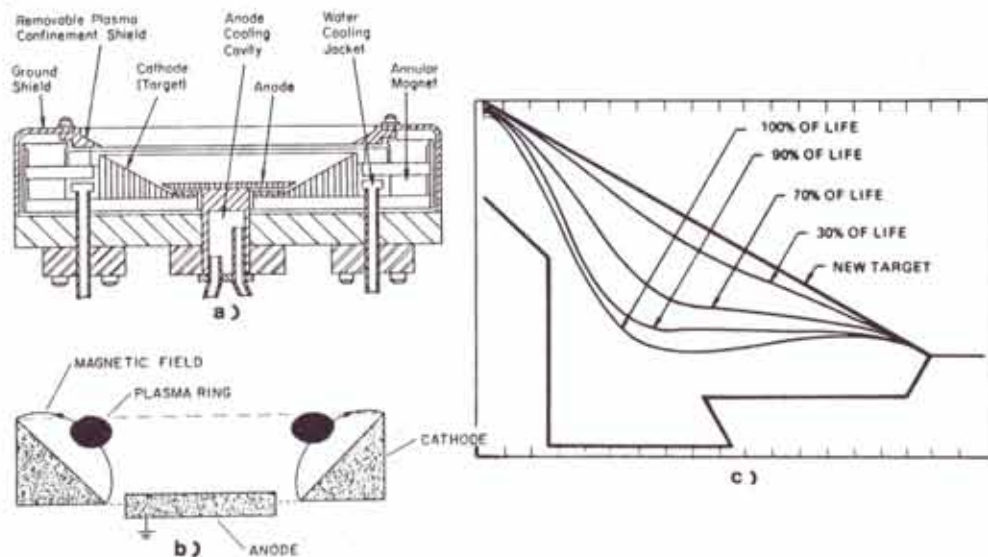


Fig. 23 Conical magnetron target and magnet configuration. Courtesy of Varian Associates.

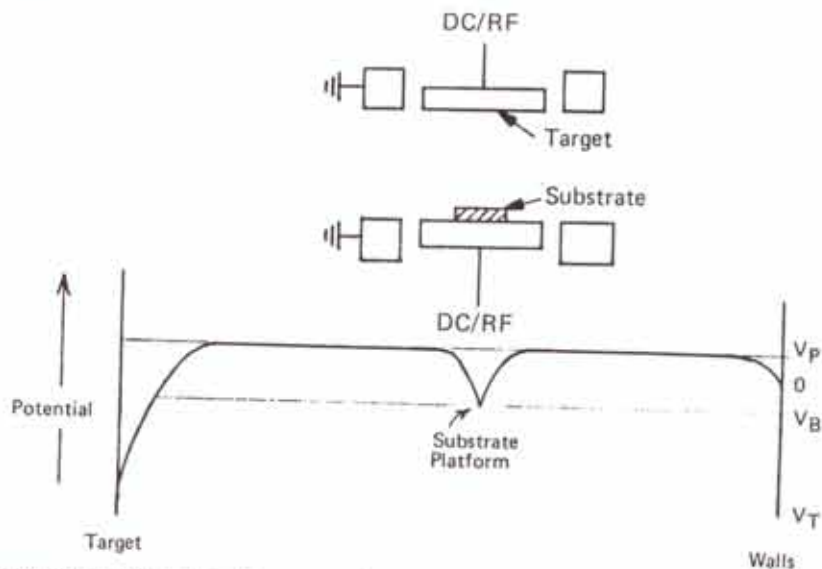


Fig. 24 Potential distribution in bias sputtering systems. From B. Chapman, *Glow Discharge Processes*, 1980 Copyright © John Wiley & Sons. Reprinted by permission of John Wiley & Sons

bombardment by positive ions. This bombardment may cause sputtering of the substrate surface. The value of the potential difference between the plasma and substrate can be left uncontrolled. If, however, the substrates are deliberately given a *negative bias* with respect to the plasma (usually smaller than the negative bias applied to the target), this *bias sputtering* effect can be harnessed to modify some of the properties of the films deposited on the substrates<sup>4,15</sup>. Most commonly, an rf bias on the substrate is used, with dc or rf power applied to the target.

In Fig. 24a, it is shown how the substrates in such a configuration are electrically isolated from ground, and biased. In Fig. 24b the potential distribution of the configuration is illustrated. Since this arrangement allows the bias voltage on the substrate to be adjusted, this also permits the flux and energy of electrically-charged particles striking the substrates to be varied. In fact, use of bias sputtering enables a large number of film properties to be controlled including gas incorporation, step coverage, stress, reflectivity, grain size, resistivity, surface roughness, hardness, and alloy composition.

As an example, Winters and Kay<sup>16</sup> measured the incorporation of Ar in a growing Ni film as a function of substrate bias (Fig. 25). For low bias voltages less Ar was found in the films, because incoming Ar ions sputtered the previously sorbed Ar, but did not embed themselves in the film. An increase in the bias voltage, however, also raises the kinetic energy of the impinging ions. Thus, they eventually become energetic enough (at  $\sim 100$  eV) to occasionally be implanted into the growing film. For energies greater than this value, the implantation effect becomes increasingly dominant, and the percentage of incorporated Ar starts to rise again.

The bias voltage can also impact the film properties in several other ways including: a) the incoming ions add energy to the surface ions and thus increase surface migration or chemical reaction rates at the surface; b) if the ions possess sufficient energy ( $\sim 100$  eV), resputtering of the deposited film atoms can occur; c) the incoming ions can damage the surface of the growing film; and d) the growing film can be heated by the ion bombardment. All of these mechanisms



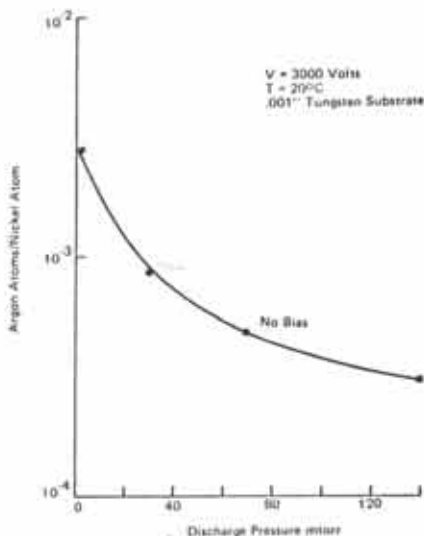


Fig. 25 Argon content in sputtered nickel film as a function of argon discharge pressure<sup>16</sup>. Reprinted with permission of the American Physical Society.

can alter the properties of the growing film, often in unexpected ways. References 4,17,18,31,35 describe how bias sputtering has been used to modify a variety of specific film properties.

## Sputter Deposition Equipment

A large and stringent set of material properties must be exhibited by VLSI interconnect films. In order to successfully deposit such films by sputtering, complex and sophisticated sputtering systems must be utilized. These are offered commercially in a variety of configuration designs. Each has certain advantages and limitations, and it is up to the user to determine the best equipment type for specific applications. In this section we discuss the various equipment types, after first describing the generic components of a VLSI fabrication sputtering system.

Before discussing the details of sputtering equipment, it is useful to list the most important requirements of VLSI interconnect films, and the equipment used to deposit them. The necessary film properties, and how they are achieved by various sputtering processes, are the subjects of a later section. The requirements placed on sputter deposition equipment will be explored here.

In general, there are some desired qualities shared by all processing equipment including: a) safe operation; b) adequate process throughput; c) compatibility with the required processes to be performed; and d) compatibility with the VLSI manufacturing environment. Let us see what attributes need to be possessed by sputtering equipment to meet goals (b), (c), and (d), as any machine not capable of safe operation would automatically be disqualified.

The *throughput* of a sputtering system depends on such factors as: maximum deposition rates; single-wafer vs. batch operation; pumpdown times; pre-processing cycle times; reliability (i.e. percentage uptime of equipment); and scheduled maintenance requirements (e.g. time between regeneration of cryopumps, or time between target replacement). In general, magnetron sputtering with power supplies capable of supplying high power and optimally designed targets

are utilized to maximize deposition rates.

The *process compatibility* characteristics of a sputter system involve such questions as: a) should the system be flexible or not? (i.e. will it be called upon to deposit a wide variety of materials, multilayers, etc., or will it only be dedicated to a narrowly defined set of sputter depositions?); b) what size wafers can the system handle?; and c) can the system perform all the aspects of the desired processes, such as sputter etching, wafer heating, dc or rf magnetron sputtering, rf diode sputtering, or bias sputtering?

The *compatibility with the VLSI manufacturing environment* addresses the following issues: a) compatibility with clean-rooms (i.e. the systems must be clean, should occupy as small a space as possible in the clean-room, and ought to be serviceable from outside the clean-room); b) capability of interfacing with factory automation-computer systems; and c) compatibility with robotic loading and unloading.

The schematic of a sputtering system is shown in Fig. 26. It consists of the following components: a) sputter chamber, in which reside the electrodes and sputtering targets and possibly shutters; b) pre-processing chamber, which may contain wafer heaters, rf sputter etch electrodes, and also function as a load-lock; c) vacuum pumps; d) power supplies (dc and /or rf); e) sputtering targets; f) sputtering gas supply and flow controllers; g) monitoring equipment (pressure gauges, voltmeters, and residual-gas analyzers); h) wafer holders and handling mechanisms; and i) microcomputer controller. We will present information only on items (a), (b), (c), (d), and (e), as these components operate somewhat differently in sputtering systems than in other equipment. The remaining subsystems, on the other hand, play the same role in sputtering systems as they do in many other semiconductor equipment applications.

The *sputter chamber* (and its associated subcomponents), not only make up the heart of a sputtering system, but each design is also the most unique part of the commercial systems. Therefore we will delay the discussion on sputter chambers until the various system configurations are compared.

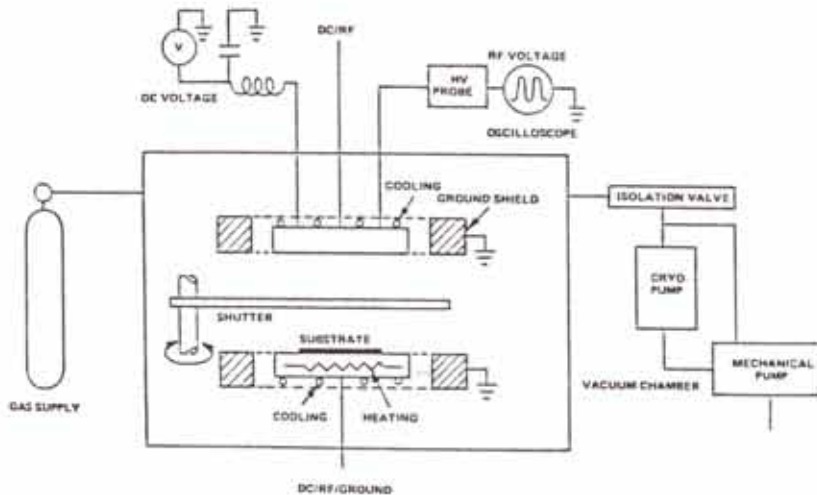


Fig. 26 Schematic drawing showing some of the components of a sputtering system.

The *pre-processing chamber* (or *station*), is normally a chamber into which the wafers are first transferred from the ambient. Several procedures may be conducted in the pre-process chamber (PPC), depending on the system design, including: a) pumpdown of the PPC; b) heating of the wafers; and c) cleaning of the wafer surface by sputter etching or other means (e.g. plasma etching). The purpose of the *pumpdown* is to allow the sputter chamber to be loadlocked (i.e. wafers can be introduced into the sputter chamber without requiring that it be vented to atmosphere). After the deposition is completed, the wafers can be transferred through the same PPC, or another loadlock chamber, and brought out of the system. The sputter chamber itself is normally kept under high vacuum when sputtering is not taking place. *Wafer heating* may be used to accomplish several purposes, including desorption of moisture, etc., from the wafer surfaces, and/or preheating to improve step coverage during deposition. In some systems, however, such step coverage heating may be done in the sputter chamber during deposition.

The *vacuum pumps* are also an important part of the sputtering system. For cleanliness sake, most sputtering equipment manufacturers have opted to use cryopumps to keep the sputtering chamber under high vacuum between times of sputtering<sup>19</sup>. This pump is normally also used during the sputter process to continually pump the chamber (at pressures  $\sim 1$  Pa). In order to use high vacuum cryopumps to maintain such medium vacuum pressures, the pump must be throttled, and this reduces its pumping speed. Since the purpose of pumping during a sputter process is to remove evolving gas contaminants (especially moisture) on a continuous basis, the reduction of pumping speed is undesirable. Thus, *Meissner traps*<sup>20</sup> (described in Chap. 3) are sometimes placed in sputter chambers to maintain high water vapor pumping speed. Some systems are also offered with *titanium sublimation pumps* for gettering the large volumes of hydrogen evolved in the chamber during sputtering (i.e. from residual moisture on wafers and holders that dissociates into H and O, and from the  $H_2$  absorbed in stainless steel chamber fixtures). This allows the cryopump to be operated for longer periods between regeneration, as saturation with  $H_2$  is usually the condition that mandates pump regeneration<sup>20</sup>.

The vacuum in the loadlock PPC may be created by a rough pump or turbomolecular pump. Some reports indicate that the loadlock should be pumped to  $<1$  mtorr in order to prevent excess  $N_2$  from being introduced into the sputter chamber from the PPC<sup>20</sup>. This would require a high vacuum pump to evacuate the loadlock.

The *power supplies* in a sputtering system may be dc or rf. Dc power supplies can be built to supply up to 20 kW of power, whereas rf power supplies are limited to  $\sim 3$  kW. As a result, dc magnetron sputtering can provide higher deposition rates than rf magnetron sputtering, and consequently is the operational mode of choice for high deposition rate processes. Dc power supplies for sputtering, however, must be designed to be capable of withstanding arcs without damage<sup>12</sup>. Such arcs are thought to arise from the local dielectric breakdown of native oxides on freshly installed targets, or from other surface regions on which contaminant insulator layers have formed. Conversely, rf sputtering removes such regions as a matter of course, and thus rf supplies are not subjected to arcing. The dc supplies, however, must be designed to handle such local arcing without shutting down or damage, as the regions responsible for such arcing are normally cleaned within minutes after the power is supplied to the system, and arcing then ceases. On the other hand, the supply must be able to sense large arcs caused by such events as metal flaking between the target and ground, and to be able to switch off soon enough to prevent damage to the target. Saturable reactor power supplies are used for dc magnetron applications, as they are tolerable of arcs, and yet can maintain a constant current output for a wide range of loads. When bias sputtering is carried out, a separate supply may be provided, or power from a single

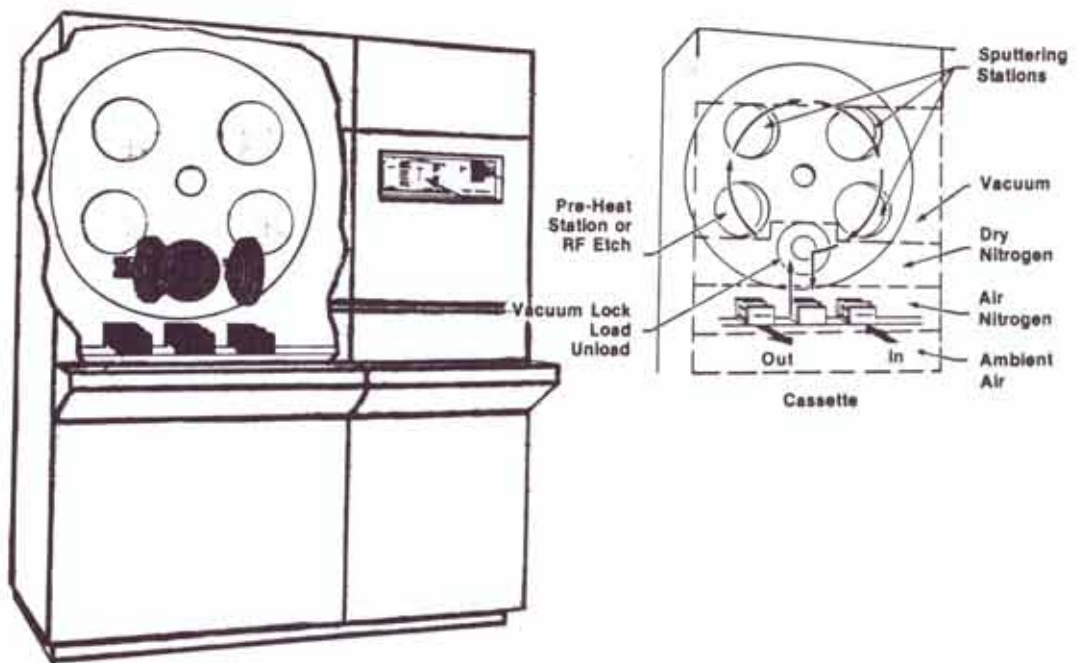


Fig. 27 Static sputtering system, Varian 3180. Courtesy of Varian Associates.

supply may be split and fed to both target and substrate electrodes at the required voltage and phase difference.

The *target* consists of the material that is to be sputter-deposited onto the substrate. Target shapes depend on the material to be deposited and the sputtering system design. Figure 21 shows some of the target shapes in common use<sup>21</sup>. Sizes range from round targets only a few inches in diameter, to rectangular targets several feet long. Targets are mounted to the cathode in such a way that they are in intimate contact with a water-cooled backing plate. Since it is estimated that over 70% of the energy incident on the target goes into heating, targets must be adequately cooled to prevent warpage, deposition rate changes due to thermal restructuring, or even melting. Most metal targets are fabricated from high-purity, vacuum cast materials (e.g. 99.999 - five nines, 99.9995 - five nines five, or 99.9999 - six nines pure, for aluminum targets, as four nines purity is generally unacceptable for semiconductor metallization). Some applications also demand material that is very low in alpha-particle emitting elements (e.g. low thorium and uranium content). Other desirable characteristics of targets include: high percent utilization of the target material; the ability to perform a large number of runs between target replacements; and accurate alloy composition. *Composite targets* consist of two or more metals in unalloyed form with a selected ratio of surface areas mechanically arranged, so that sputtering takes place simultaneously to yield an alloy in the deposited film.

Presputtering of targets is done to clean their surfaces prior to film deposition. Shutters may be used to protect wafers present in the chamber from being deposited with the target surface contaminants, during such target cleaning. Once the target surface is clean, sputter deposition

can be initiated. As discussed in the power supply presentation, arcing may occur at the target surface in dc sputtering until the surface is cleaned. Thus, it is common practice to *condition* freshly installed targets by slowly increasing the applied power, until all the material that causes the arcing has been sputtered away.

### Commercial Sputtering System Configurations

The systems commercially offered for VLSI sputtering applications<sup>29</sup> differ primarily in the design of the sputter chamber, electrode arrangement, and wafer-target relationship. Note that virtually all systems have load-locked sputter chambers, and offer wafer heating, rf sputter etching, and bias-sputter deposition capabilities. The following are examples which represent most of the variations offered in sputter system design. They are:

a) The *static* sputter configuration (Fig. 27), in which the electrodes are in an S-gun<sup>®</sup> (or Sputter gun<sup>®</sup>) configuration, and the wafers (normally smaller in diameter than the S-gun cathode) are placed within 5-10 cm of the target<sup>13</sup>. Only one wafer at a time is sputter deposited from each target, and the wafer and the target are held in fixed positions during the deposition, hence the name, *static deposition*. Note that systems may have more than one sputter station, so that several wafers may be sputtered simultaneously, and multi-layered films can be deposited by moving a wafer between stations. Normally, the wafer is held vertically, and this positioning is known as *side-sputtering*. In such systems, each wafer can be individually heated during deposition. Advanced S-gun, circular magnetron configurations have been designed to allow large diameter wafers (150-200 mm) to be deposited with films possessing  $\pm 5\%$  thickness uniformities.

b) The *in-line sputter* configuration (Fig. 28)<sup>5,11</sup>, in which the wafers travel in a straight

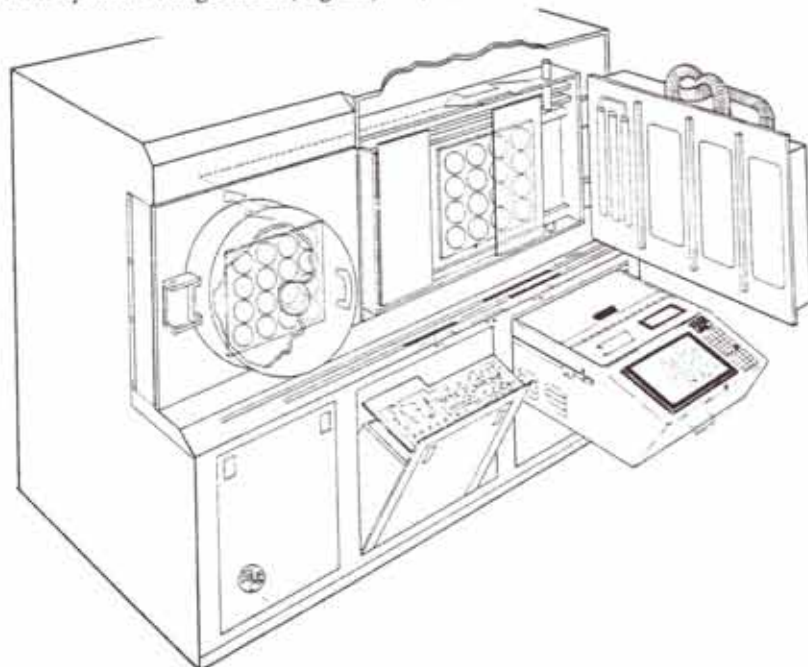


Fig. 28 MRC model 603 in-line side sputtering system. Courtesy of MRC.

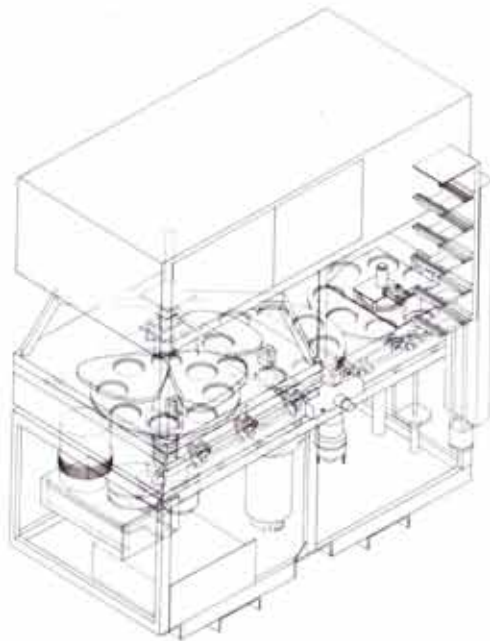


Fig. 29 Planar rotation sputtering system. Courtesy of Gryphon Products.

path and in front of a rectangular shaped planar magnetron target (Fig. 21b & 22). Normally the deposition occurs as the result of a single pass, but multiple passes under the target can also be performed, if desired. In such systems, the deposition rate is determined, and then the transit speed in front of the target is adjusted to yield the desired film thickness. Such systems are batch systems, and the number of wafers per batch is dependent on the wafer diameter. In-line systems can contain more than one sputtering station. This allows several types of materials to be deposited without having to change targets, or to deposit multilayered structures in one vacuum pumpdown. Wafers are again held vertically, and thus side-sputtering is used.

c) In *rotating platter*<sup>20,23</sup> sputter systems (Fig. 29 & 30a) the wafers make multiple passes in front of the planar magnetron target, as the platter on which they are mounted rotates. Such systems are batch systems, and the size of the batch depends on the wafer diameter, although most systems have a maximum wafer size that can be accommodated. Multiple targets can be used, so that multiple layer films can be easily deposited in a number of various structures (e.g. layered films of Al-Si and Ti, which are reported to prevent hillock formation). The target, typically wedge-shaped as shown in Fig. 21a, can be above or below the wafers. In most rotating platter systems (Fig. 30), the wafers pass below the wafer target (sputter-down mode). For processes in which spalling and flaking result in large particle generation (i.e. Ti:W or silicide process film depositions), this configuration would not be feasible, as the particles would fall onto the wafers. For aluminum depositions, or multi-layer depositions in which underlying

Ti:W layers are immediately covered with Al, the films are highly adherent. Any micrometer size particles that might exist in the sputter environment, are directed by electric fields, and not by gravitational fields. Hence, it is claimed that the spatial orientation of the sputtering process is not relevant, and that sputter-down systems produce no more particles on wafers than do systems which sputter up or sideways. The combination of rotary motion, target design, and heating has been reported to produce enhanced step coverage in Al films with some of these systems.

d) In *rotary drum* sputter systems, wafers are mounted on the surface of a rotating cylinder, and make multiple passes in front of planar magnetron targets as the cylinder or drum rotates. The principle is similar to the in-line systems, except that the motion is rotary rather than linear. If multiple passes before the target are advantageous to a process (compared to a single pass, or vice versa), the rotary versus in-line configurations offer a choice. Side-sputtering is used in most drum type systems.

### Process Considerations in Sputter Deposition

The goal of a deposition process for producing an interconnect layer is to create a film having all of the properties required for the VLSI technology that is being fabricated. In this section, we list the desirable properties of an interconnect film and discuss factors that impact the quality of such characteristics. Some of the relevant information was presented earlier in the sputtering discussion, but other practical considerations still need to be addressed.

A deposited interconnect film must satisfy a large number of requirements in order to effectively perform its role in an integrated circuit. (Note that the film properties necessary to meet these requirements must be exhibited by both sputtered and evaporated films.) A "wish list" of some of the most important of these characteristics that depend on the deposition process includes: a) correct nominal thickness; b) thickness uniformity of at least  $\pm 5\%$  (across the wafer, and wafer-to-wafer); c) low resistivity; d) uniform resistivity of at least  $\pm 5\%$ ; e) good adhesion to underlying and overlying layers; f) good step coverage (e.g. usually  $>50\%$  is desired); g) high electromigration resistance; h) good resistance to hillock formation; i) controllable reflectivity; j) film hardness is controllable to a desired specification, for wire-bonding compatibility; k) the layer can make low-resistance contacts to Si and/or other interconnect layers; l) the films can be

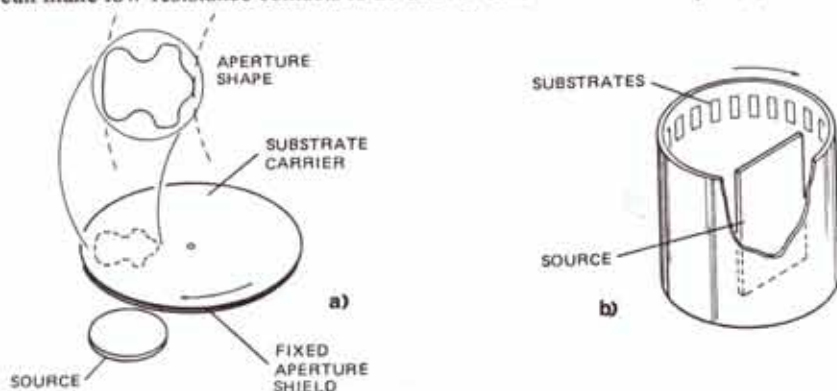


Fig. 30 Planar magnetron deposition with substrate motion: (a) planar rotation with aperture shield. (b) drum rotation<sup>39</sup>. Reprinted with permission of Academic Press.

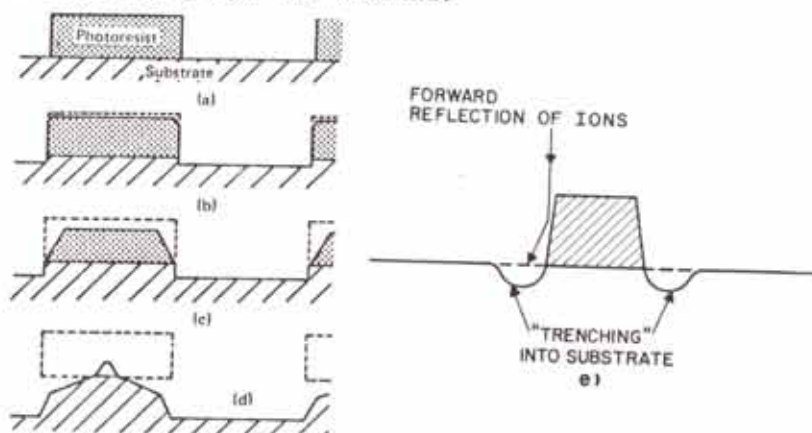


Fig. 31 Faceting results from the dependence of sputter etch rate on the angle of incidence of ions striking the surface. (a) prior to etching, (b) initiation of the facet, (c) facet intersects the substrate surface, (d) substrate is exposed and forms its own facet. (e) Trench formation arises from an excess flux of ions resulting from reflection off the sidewall. Copyright, 1983, Bell Telephone Laboratories, Incorporated, reprinted by permission.

deposited as an alloy with tightly controlled composition; m) the film may be required to possess a multilayer structure; n) grain sizes in the film can be controlled; o) deposited films are low in alpha-particle emitting elements (uranium and thorium); p) stresses in the deposited film are low; and r) there is a reasonable latitude in the process conditions that effect the desired film properties.

In the following discussion we will focus on the aspects of the sputtering process that impact many of the above properties, especially, alloy composition, step coverage, resistivity, hillocks, electromigration, hardness, stress, and reflectivity. Additional information on stress, adhesion, and resistivity of thin films is found in Chap. 4, and a detailed discussion of electromigration and hillocks is undertaken in Vol. 2 of this text.

### Faceting and Trenching

Faceting and trenching are two effects arising from sputtering that can impact the results of sputter etch processes, as well as the reactive-ion etching processes discussed in Chap. 16.

The effect of *faceting* is illustrated in Fig. 31a-d, in which the sidewall of a feature is seen to develop an increasingly larger facet as the sputtering continues. (The term *facet* originated as a description of the *small faces* that are cut from the surface of a jewel.) The faceting effect arises from the fact that sputtering yield is greater from surfaces which are inclined at a non-90° angle to the incoming ions (Fig. 9). The facet usually starts on corners, which always have some rounding, but is also more pronounced in bias-sputtering processes due to the increased electric field at sharp corners. The facet is inclined in the direction of the incident angle corresponding to the angle of maximum sputtering yield. The faceting effect can *directly* alter substrate step profiles if an unprotected substrate is sputter etched. On the other hand, as shown in Fig. 31a-d, if a protective layer (e.g. photoresist) is used during a sputter etch or RIE process, the facet developed in the masking layer can still be *indirectly* transferred into the etched film, if the etching proceeds long enough that the facet intersects the surface.

The phenomenon of *trenching* is illustrated in Fig. 31e. It stems from the enhanced ion



flux at the base of a step due to ion reflection off the side of the step, which causes etching to occur more rapidly there.

### Wafer Heating During Sputter Deposition

Heating of the wafers can occur during sputter deposition. This heating may be a natural consequence of the process, or may be deliberately produced by auxiliary heating procedures. In some cases heating produces beneficial effects, especially if it can be controlled, while in other instances the heating can degrade the deposited film properties.

Unintentional heating is primarily caused by the following: a) high-energy electrons striking the substrates; b) the heat-of-condensation of the depositing film (this component is more important in high deposition rate processes); and c) the kinetic energy of the arriving film atoms. In magnetron sputtering, fewer high energy electrons escape from the target region to strike the substrates, and electron capture shields are utilized to suppress this effect even further. Thus, in modern sputtering systems, this heating effect has been significantly reduced. The heat of condensation and kinetic energy of the incoming film atoms will cause only small temperature increases in low-deposition-rate processes, while in high deposition-rate processes (e.g.  $1 \mu\text{m}/\text{min}$  Al depositions), temperature increases of  $-50^{\circ}\text{C}^{24}$  to  $100^{\circ}\text{C}^{25}$  have been reported.

Heating by auxiliary means to improve film properties (e.g. step coverage), is conducted by lamps, backside heating with hot Ar gas, and other techniques. It should be noted that although it is difficult to measure the exact temperature on the wafer surface during deposition, in practice it is possible to reproduce the same heating from run-to-run.

### Deposition of Alloy Films

In many sputter deposition applications, it is desired that alloys, rather than pure films be deposited (e.g. Al-alloys, or Ti:W). They may be deposited by co-sputtering from multiple targets, but it is more common that single, multicomponent targets are used. In steady-state sputtering conditions, the elements are sputtered from the target in the same ratio as are present in the alloy. Let us discuss the mechanism associated with such single target depositions that causes the composition of the sputtered film to track that of the target alloy composition<sup>4,15,21</sup>.

When the surface of a metal alloy is initially exposed to the impinging ions in a sputter process, it will have its nominal composition (e.g. 2at%Cu: 98at%Al). Since Cu has a slightly higher sputter yield than Al (e.g.  $\sim 2.7$  vs.  $\sim 2$ , for 1000 keV Ar ions), the ratio of Cu to Al atoms sputtered would be higher than the ratio of Cu to Al in the target, if 1000 keV ions are used. But this situation would not persist for very long. As the surface gets relatively depleted of Cu, the sputtering rate of Al atoms increases (and that of Cu decreases), until in the steady-state, the material is leaving the surface in the ratio of 2Cu : 98Al. It is useful to use a shutter during the period in which the surface concentration is stabilizing, to prevent deposition of material with non-desired alloy composition onto the substrate.

The composition of the deposited film, however, may not exactly mirror the composition of the target because of other factors. For example, if the alloy constituent atoms differ greatly in mass, the lighter atoms will be more strongly scattered by Ar atoms as they move from the cathode to the substrate. In addition, if bias-sputtering is utilized, resputtering of the deposited film may alter the film composition (often in unexpected ways). Thus, the film composition must be measured for each process condition. Again, once a set of process conditions is fixed, it is possible to obtain reproducible results from run-to-run.

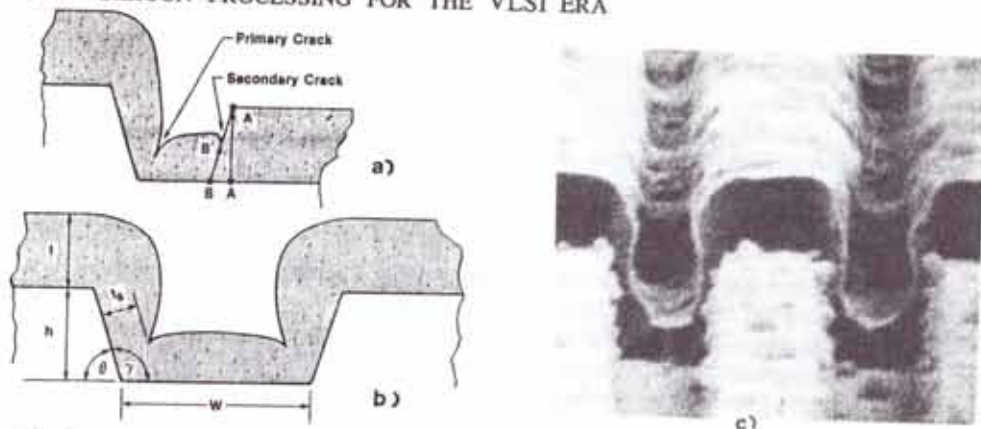


Fig. 32 Computer simulated film growth on a step: (a) Point source planetary system; (b) dc magnetron sputtering system<sup>47</sup>. Reprinted with permission of Solid State Technology, published by Technical Publishing, company of Dun & Bradstreet. (c) Example of poor metal step coverage.

### Sputter Deposition Process Control of Step Coverage

In most applications it is desired that thin films maintain a uniform thickness and freedom from cracks or voids. As thin films cross steps that occur on the surface of the underlying substrate, they may suffer unwanted deviations from the ideal, such as thinning or cracking<sup>47</sup>. A measure of how well a film maintains its nominal thickness is expressed by the ratio of the minimum thickness of a film as it crosses a step,  $t_s$ , to the nominal thickness of the film on flat regions,  $t_n$  (Fig. 32). This film property is referred to as the *step coverage* of the film, and is expressed as the percentage of the nominal thickness that occurs at the step:

$$\text{Step Coverage (\%)} = (t_s / t_n) \times 100\% \quad (13)$$

Step coverage of 100% is ideal, but each process is normally specified by a lesser minimum value that is acceptable for a given application. It is important, however, that the circuit designers understand the actual step coverage value, and derate the maximum allowable current in an interconnect line to reflect the step coverage limitation. The height of the step and the *aspect-ratio* of the feature being covered, also determine the expected step coverage. That is, the greater the height of the step, or the aspect ratio (i.e. the height-to-spacing ratio of two adjacent steps), the more difficult it is to cover the step without thinning of the film, and hence the worse the expected step coverage. Besides the step height and aspect ratio, the step coverage depends on two other factors which are not controllable by the sputtering process: 1) the *shape*; and 2) the *slope*, of the step. In general, the smoother the contour and the smaller the slope of the step, the better the expected coverage. Assuming that the four above factors have been fixed as a result of previous process steps, there are then several conditions of the sputtering process that can be adjusted to improve step coverage, including: a) sputter etching the underlying substrate prior to film deposition, to reduce the slope of surface steps; b) optimization of the target design; c) substrate heating; and d) substrate-bias sputter deposition.

One purpose of *sputter etching* of the substrate surface is to reduce the severe slopes of the steps. This phenomenon makes use of faceting effect described earlier. It should be noted, however, that much more material from the surface layer must be removed to achieve significant

slope-reduction of steps, than is removed during the more common sputter-etch steps that remove thin [ $\sim 50\text{\AA}$ ] native oxides. The utilization of this effect to enhance step-coverage in a three-level metallization process is discussed in Ref. 27.

By optimizing the *shape of the target* and by *controlling the target regions where maximum sputtering occurs*, step coverage can also be enhanced. The details of such target and related system design practices are generally unique to each sputtering system, and some designs are apparently more effective at improving step coverage than others. The general idea is that the extended source configurations of the sputtering systems can offer the potential of such improvements. As progress is continuing to be made in this area, it will be up to users to monitor the claims of enhanced performance by equipment suppliers, and decide for themselves which improvements can best benefit their processes.

*Heating the substrate* has been shown to improve step coverage<sup>20</sup>. This effect occurs because the migration of the surface atoms of deposited films increases with substrate temperature (Fig. 33a & b). As a result, the atoms tend to move toward regions where the least amount of material has been deposited, thereby averaging out the film thickness (i.e. the concentration gradient of material favors diffusion toward less populated locations). For aluminum films, the substrates must be heated to  $>250^\circ\text{C}$  before significant coverage improvements are observed. It has been postulated that intermittent deposition, or thin  $\sim 200\text{\AA}$  thick films (e.g. from multiple passes before the sputter target) is especially effective. That is, during the times that the heated film is not being coated, surface atoms are given the opportunity to migrate. If they are sufficiently mobile, they will equalize their distributions across the surfaces. The optimum temperature and deposition parameters will depend on the particular step topography, and must be determined for each process. An understanding of surface migration phenomena is necessary for developing adequate models of this mechanism. It should also be noted excessive heating during deposition can cause hillock formation in Al films. Thus, the step-coverage heat cycle often represents a compromise temperature. This effect also emphasizes the importance of being able to control the temperature.

*Bias-sputtering* (introduced earlier) is another technique that has been utilized to increase step coverage of deposited films (Fig. 34)<sup>23,26</sup>. That is, an rf bias is applied to the wafers, causing them to be bombarded by energetic sputter gas ions (e.g.  $\text{Ar}^+$ ), as the film is being deposited.

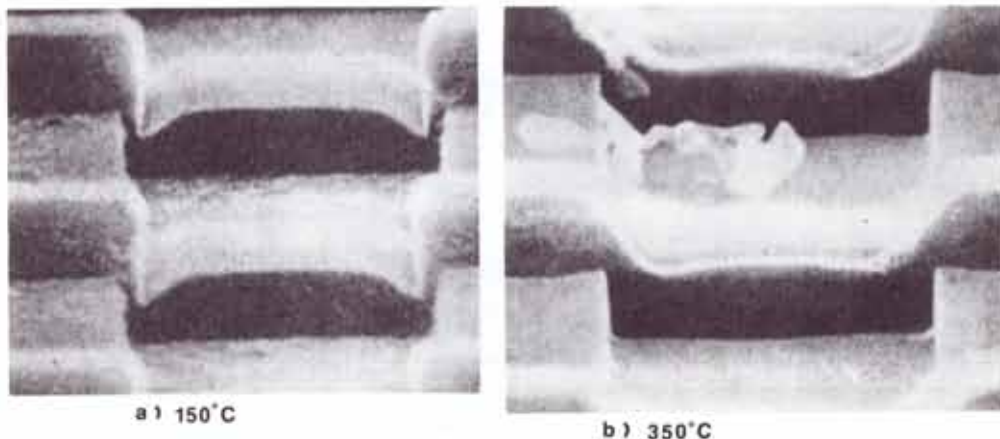


Fig. 33 Effect of heat on step coverage. Courtesy of Varian Associates.

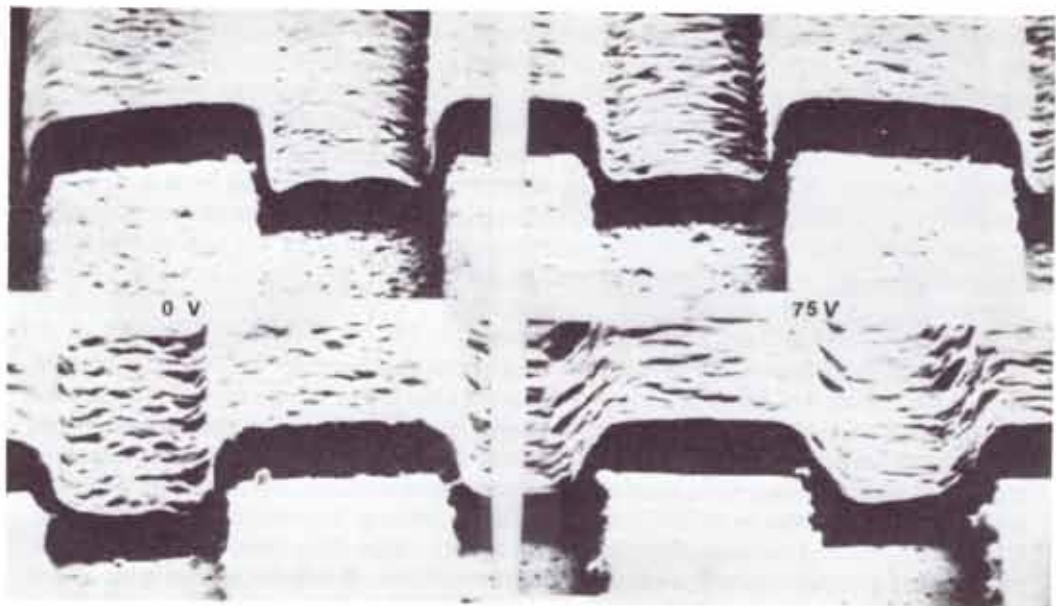


Fig. 34 Effect of different bias voltages on sputter deposited films. Courtesy of MRC.

The applied rf causes the wafers to acquire a negative self-bias, and thereby accelerates ions from the discharge toward their surfaces. The impinging ions transfer energy to surface atoms, and cause them to be transported to the sidewalls of steps, where they accumulate and locally increase the film thickness. Two mechanisms have been suggested as being responsible for such atomic transport: a) the transferred energy from the bombarding ions increases *surface atom migration*, thereby improving step coverage (much as in substrate heating); and b) the transferred ion energy causes *re-sputtering from the surface of the depositing film*<sup>35</sup>. Since the directions of the atoms emitted in such re-sputtering is thought to occur according to an

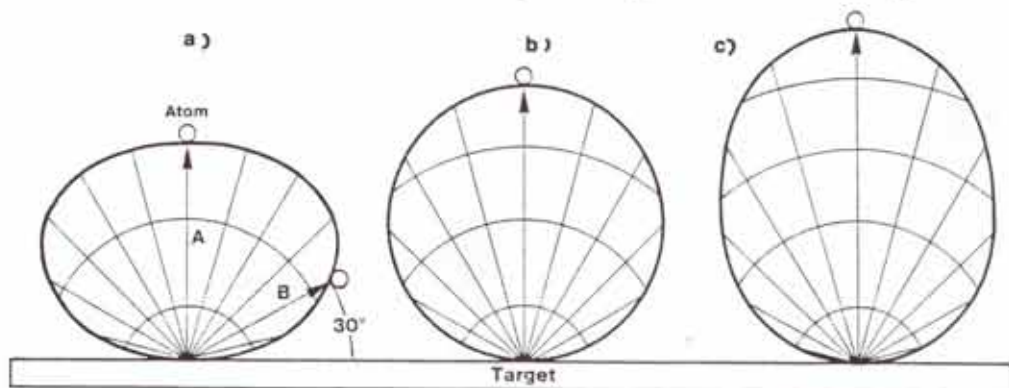


Fig. 35 (a) Under-cosine emission distribution. (b) Cosine emission distribution. (c) Over-cosine emission distribution.

*under-cosine* distribution (Fig. 35), more atoms will be directed at the sidewalls of steps, where they accumulate. The surface migration model enjoys more support, as it is argued that energies of impinging ions in bias sputtering appear to be too small to cause appreciable resputtering.

### Sputter Processes for Various Thin Film Materials

This section discusses process conditions used to sputter deposit a variety of films for VLSI applications, including: a) aluminum and aluminum alloys; b) titanium-tungsten; c) platinum; d) refractory metal silicides; and e) fused silica (also referred to as quartz).

*Aluminum and aluminum alloy* films of  $\sim 3000$ - $12,000\text{\AA}$  thickness are deposited by dc magnetron sputtering, since high deposition rates are normally required ( $3000$ - $10,000\text{\AA}/\text{min}$ ). Substrate heating and/or bias-sputtering are frequently used to enhance step coverage. Film reflectance and alloy composition to some degree are also impacted by bias-sputtering conditions. Residual gases (O, N, and H)<sup>46</sup> can cause deleterious effects in the deposited film. For example, in the discussion on process of film formation during sputter deposition, it was noted that small amounts of  $\text{O}_2$  can lead to large resistivity increases in the Al films. In addition,  $\text{O}_2$  can produce an increase in the film *hardness* (which can cause difficulty in forming strong wire-bonds to such hardened films). The presence of  $\text{N}_2$  has been shown to produce stress in Al films. This leads to cracking and voids, which can contribute to early failures from electromigration<sup>28</sup>.

It has also been reported<sup>20</sup> that an excess quantity of  $\text{H}_2$  present in the chamber also increases the propensity of the Al films to form hillocks (Fig. 36). In addition, the pumping of large volumes of  $\text{H}_2$  will cause the cryopump to saturate more quickly, requiring increased system down-time to regenerate the pumps.

To minimize problems from residual gas incorporation, some or all of the following procedures are utilized: a) the chamber is pumped to a low base pressure before being back-filled with Ar at the start of the deposition process; b) the wafers and wafer holders are pre-heated in the load-lock chamber to desorb surface moisture; c) high purity Ar gas is used; d) in some systems Ti sublimation pumps are offered for pumping  $\text{H}_2$ ; e) residual-gas analyzers are used to monitor the gas composition during the sputter process; f) the chamber is pumped during the process with a high-throughput pump (e.g. cryopump and Meissner trap) so that the residence time of any desorbing contaminant gases is short; and g) high deposition rate processes are used, so that the

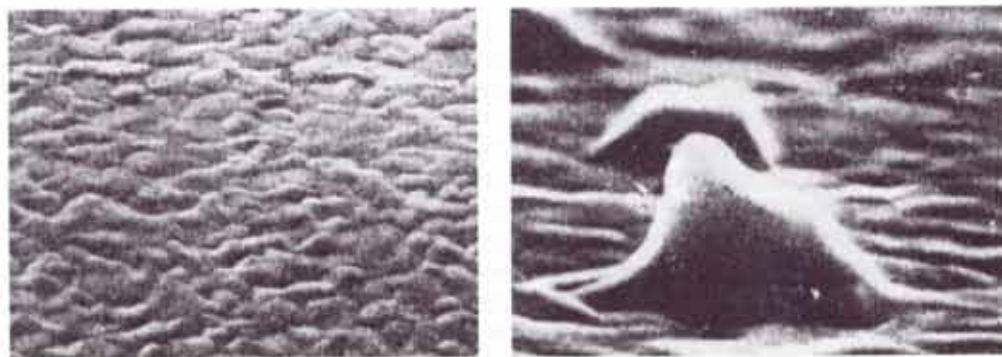


Fig. 36 Comparison of hillock-free and hillock containing films.

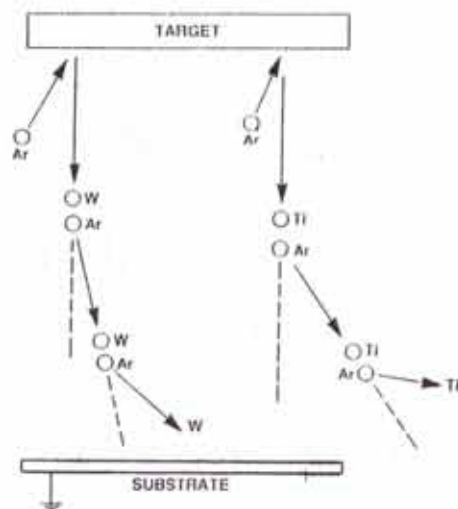


Fig. 37 Titanium-tungsten gas scattering model. Courtesy of MRC.

growing film is exposed to any impinging contaminant gases for the shortest possible time.

*Aluminum alloy films* are usually deposited from a single compound target, but successful deposition by co-sputtering has also been reported, especially if the alloy material is to be introduced as a series of thin layers<sup>20,23</sup>. In many cases, an underlying layer (e.g. Ti:W), or overlying layer (e.g. TiSi<sub>2</sub>) is applied during the same pumpdown, and in such instances the sputtering system must have the capability of depositing several materials in a single process.

*Titanium-tungsten* is also deposited using magnetron sputtering (dc or rf). The deposited film contains less Ti than the target alloy (~50% less), since the Ti atoms are lighter than W, and are strongly scattered by the Ar gas atoms (Fig. 37). The trajectories of the heavier W atoms, on the other hand, are less perturbed by collisions with Ar. As a result, more of the scattered Ti ends up on the chamber walls, and less on the substrate. (Thus, to get a film of 10% Ti, 90% W, by weight, a target containing ~19% Ti must be used.<sup>30</sup>) This effect has two important implications: 1) the resistivity of the deposited film depends on the Ti concentration since  $\rho_{Ti} = 48 \mu\Omega\text{-cm}$ , and  $\rho_W = 5.5 \mu\Omega\text{-cm}$ . In some applications the resistivity of the Ti:W film is a critical parameter<sup>31</sup> (e.g. in fuse links of some memory devices); and 2) the back-scattered Ti atoms form dendrites on the target, which eventually flake off<sup>30</sup>. A sputter-sideways technique must therefore be used in systems that are dedicated to Ti-W deposition, so that these flakes fall down in the space between the target and substrates (and not on the substrates). It has also been found that the addition of N<sub>2</sub> into the chamber during Ti:W deposition both increases the diffusion-barrier properties of Ti:W films and alters the film resistivity. If N<sub>2</sub> is added (e.g. by using pre-mixed N<sub>2</sub>: Ar gases), and the second film cannot tolerate substantial nitrogen partial pressures, a high-vacuum pumping step must be used between sequential deposition steps (e.g. Al following Ti:W). The intrinsic stress and resistivity in Ti:W sputter deposited films can also be controlled by altering the Ar pressure and bias-sputter voltage levels<sup>31</sup>.

*Platinum* is normally used in VLSI applications to form a PtSi layer in Si/PtSi/Ti:W/Al contact structures (see Vol. 2 for more details on such contact structures), and to form Schottky diodes. The Pt layers required for these uses are very thin (e.g. 500Å). In order to controllably

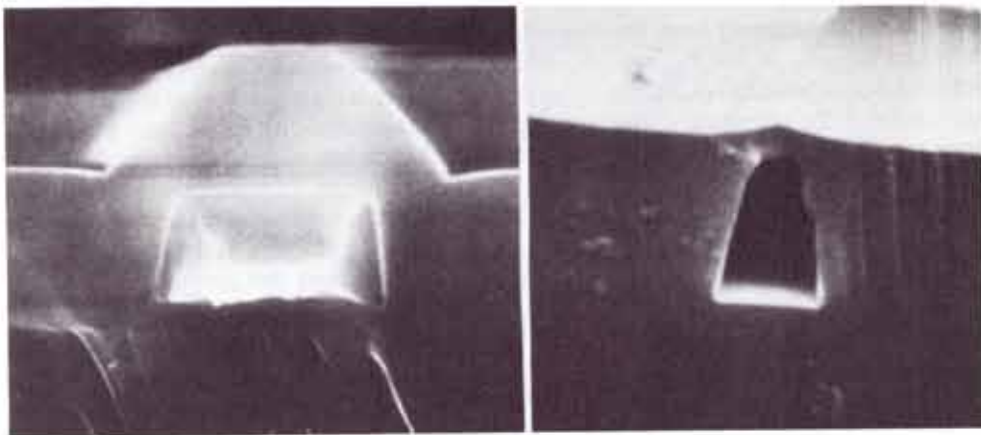


Fig. 38 Partially and fully planarized bias sputtered quartz films. Courtesy of Temescal.

deposit thin layers, a slower deposition method than dc magnetron sputtering is advantageous. Thus, sputtering of Pt is usually carried out using an rf diode or rf magnetron configuration.

*Refractory metal silicides* (e.g. Me(metal)Si<sub>x</sub>) is the desired silicide film, where x for the best quality is determined experimentally, and may range from ~2.0-2.6 are sputter deposited both by co-sputtering<sup>32,33,50</sup> and by sputtering from a single source (such as a composite or sintered target). In co-sputtered films, high purity targets are used, and calibration runs must be conducted to measure the deposition rate vs. power for each target. Then x is measured in the deposited films, and the procedure is adjusted until desired values of x are obtained. In compound target processes, several targets of different composition must be initially purchased to home-in on the best value of x. There is still some question, however, as to how reproducibly vendors will supply targets so as to maintain the necessary x in the deposited film from target to target. Bias sputtering is also normally used to promote good step coverage. The as-deposited sputtered silicide films are amorphous and possess high resistivities. A high temperature anneal (in Ar) is used to form the silicide and reduce the resistivity (e.g. a 1000°C anneal reduces resistivity by a factor of ~10). A full discussion on refractory metal silicides in VLSI is undertaken in Chap. 11.

SiO<sub>2</sub> is typically sputter deposited to provide dielectric layers for multilevel interconnect structures. The SiO<sub>2</sub> is rf sputtered from a silica glass target (although it is commonly, but incorrectly, referred to as a quartz target), and an rf bias is applied to the substrates as well, hence the name *bias-sputtered quartz*, or BSQ<sup>34,35,36</sup>. By this procedure, reduced slope steps in the deposited BSQ are achieved. In fact, the surface can be entirely planarized under certain deposition conditions (Fig. 38). The process, however, has several limitations, including: a) the deposition rate is quite slow (e.g. several hours generally are needed to deposit suitably planarized films of adequate thickness); b) the purity of glass targets is still an area of uncertainty; c) the SiO<sub>2</sub> deposits on chamber walls, as well as on the substrate. If these deposits get too thick they will flake off and form particulates. To avoid the problem, the system must be regularly and thoroughly cleaned. This may be a arduous task.

## Reactive Sputtering

The introduction of reactive gases into the sputtering chamber during the deposition process

allows material sputtered from the target to combine with such gases to obtain chemical compound films<sup>37</sup>. In addition, compound targets of some substances can be rf sputtered, and controlled partial pressures of reactive gases can be added to compensate for any loss of gaseous constituents of the compound if the sputtering target dissociates. Although these advantages appear to offer interesting process possibilities, the technique has not found wide application in the silicon microelectronic industry. Two examples of its use, however, do include: a) the addition of N<sub>2</sub> into the Ar ambient during Ti:W depositions, as discussed earlier; and b) in the deposition of the barrier film material, TiN<sup>54</sup>, by the sputtering of a pure Ti target with a sputter gas of Ar mixed with N<sub>2</sub>. The complexity of the mechanisms that can take place in the chamber when reactive gases are added to the Ar, and the difficulty in obtaining adequately pure compound targets, have otherwise restricted reactive sputtering to VLSI research laboratories.

### Future Trends in Sputter Deposition Processes

It appears that sputter deposition will continue to be the most important PVD process in silicon VLSI fabrication for some time. It is also likely that even more demands will be made on sputter deposition equipment as processing technology proceeds to evolve. The following are some of the challenges to equipment design that will arise: a) wafers will grow larger, and uniform films on such wafers will need to be deposited with high throughput; b) the machines will need to operate at higher levels of cleanliness (i.e. less particulate production); c) greater reliability (e.g. >90% up-time) will be expected; d) the machines will become progressively more automated and controllable from a central factory computer; e) the ability to improve step coverage or even planarize deposited films is an important capability being developed, and this feature will be avidly sought in new sputtering equipment designs<sup>51,52</sup>; f) alternative techniques to replace (or enhance) sputter etching for *in situ* cleaning of small area openings will be developed<sup>53</sup>; and g) as multilevel interconnect technologies are developed, more multilayer films (e.g. Ti:W /Al-Cu; or Ti /Al-Si /Ti /Al-Si /Ti) will be utilized. Sputter equipment will be called upon to deposit such complex films with high throughput.

## PHYSICAL VAPOR DEPOSITION BY EVAPORATION

### Evaporation Basics

Thin films can be deposited by applying heat to the source of film material, thereby causing evaporation<sup>38</sup>. If the heated source resides in a high-vacuum environment, the vaporized atoms /molecules are likely to strike the substrates (or chamber walls) without suffering any intervening collisions with other gas molecules. The rate of mass lost from the source per unit area per unit time,  $R$ , as a result of such evaporation, can be estimated from the Langmuir-Knudsen relation:

$$R = 4.43 \times 10^{-4} (M/T)^{1/2} p_e \quad (14a)$$

$$R = 5.83 \times 10^{-2} (M/T)^{1/2} p_e \quad (14b)$$

where:  $M$  is the gram-molecular mass;  $T$  is the temperature in °K; and  $p_e$  is the vapor pressure in Pa (Eq. 14a), or torr (Eq. 14b).



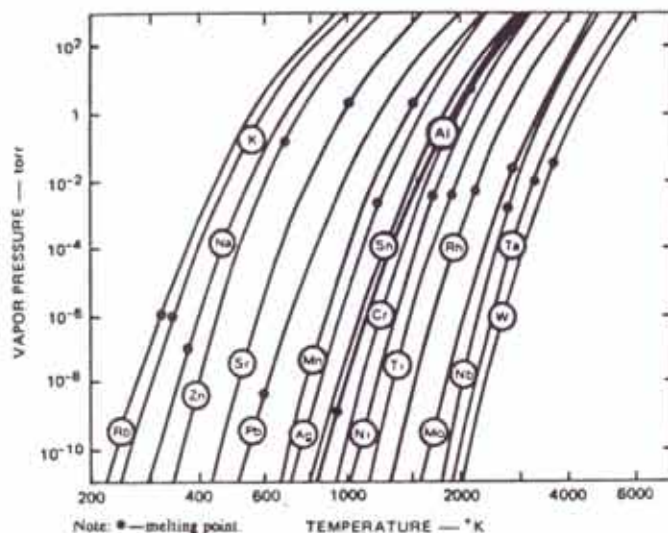


Fig. 39 Vapor pressure of metals commonly deposited by evaporation.

Figure 39 shows the vapor pressure (defined in Chap. 3) of a variety of metals commonly deposited by evaporation. To achieve deposition rates which are high enough for practical manufacturing processes, vapor pressures of  $>1.5$  Pa ( $>10$  mtorr) must be achieved. From Fig. 39 we see that there is a significant variation in the temperatures which must be applied to various materials in order to achieve such vapor pressures (e.g. Al must be heated to  $1200^{\circ}\text{K}$ , while W must be at  $3230^{\circ}\text{K}$ , before their vapor pressures exceed  $10$  mtorr).

Evaporation has been widely utilized for depositing Al and other metallic films in microelectronic fabrication. Some of the characteristics that were responsible for the widespread use of evaporation include: a) films can be deposited at high rates (e.g.  $0.5 \mu\text{m}/\text{min}$ . for Al); b) the low energy of the impinging metal atoms onto the substrate ( $\sim 0.1$  eV) leaves the substrate surface undamaged; c) due to the high vacuums under which evaporation is performed, films can be deposited with very little residual gas incorporation, and thus the deposited film is about as pure as the source material; and d) unintentional substrate heating is only caused by the heat of condensation of the depositing film, and by heat radiation from the source.

For VLSI applications, however, evaporation suffers from the following limitations: a) accurately controlled alloy compositions are more difficult to achieve with evaporation than with sputtering; b) *in situ* cleaning of the substrate surfaces is not possible with evaporation systems, but is an option in sputter systems (i.e. by performing a sputter-etch step prior to deposition); c) use of extended sources in sputter deposition can improve step coverage vis-a-vis evaporation; and d) x-ray damage, caused by electron-beam evaporation processes, is avoided in sputter deposition.

The successful deposition of thin films onto a wafer surface also implies that the following film characteristics can be achieved: a) the nominal film thickness can be controlled; b) adequate film thickness uniformity exists across the wafer; c) uniform thickness is exhibited when the

film crosses over steps (i.e. good step coverage). In evaporation processes, a different approach is used to achieve each of these three goals. To obtain the desired nominal thickness the rate of mass loss per unit area of source  $R$ , as well as data about the directions of evaporated atoms, is needed. Equation 14 can be used to calculate  $R$ . Information about the directions of evaporating atoms is more difficult to determine. The flux of atoms leaving a small area *plane source* (Fig. 40a) was theoretically postulated to exhibit a cosine distribution, and this predicts that the mass  $dM_e$  collected by an area  $d\omega$  in Fig. 40a can be calculated from:

$$dM_e = (M_e / \pi) \cos \phi \, d\omega \quad (15)$$

where,  $M_e$  is the total mass emitted by the source. Experimental information which confirmed this model was first obtained by Knudsen, who measured the evaporation from a small area plane source onto the inner surface of a sphere (Fig. 40b). In this experiment,  $\cos \vartheta = \cos \phi = r / 2r_0$  for each point on the sphere. Thus, the amount of deposit according to Eq. 15 should be uniform for every point on the sphere, and this was indeed observed. From this data, it would seem that to obtain uniform coating of wafers, it would only be necessary to mount them on an inner surface of a sphere, and evaporate from a source as shown in Fig. 40b.

Unfortunately, actual sources do not have infinitesimally small areas, but are in fact *extended* sources. Thus, the directions of emission do not follow the ideal cosine distribution. In addition, the region directly above high-rate evaporation sources is populated by evaporant atoms with a density large enough to cause them to exhibit *viscous* rather than *molecular* flow. This disturbs the directional distribution even further (Fig. 40c). As a result of these (and other non-ideal emission effects), uniform distribution at every point on a sphere surface does not occur.

The technique developed to achieve maximum uniformity during evaporation, in spite of deviations from the ideal, is to mount the wafers onto a mechanical *planetary* fixture inside the chamber (Fig. 41). During deposition, the entire fixture rotates about the vertical axis of the vacuum chamber, and each wafer is also rotated about a second axis. The combination of rotary motions results in maximum thickness uniformity across a substrate, as well as substrate-to-

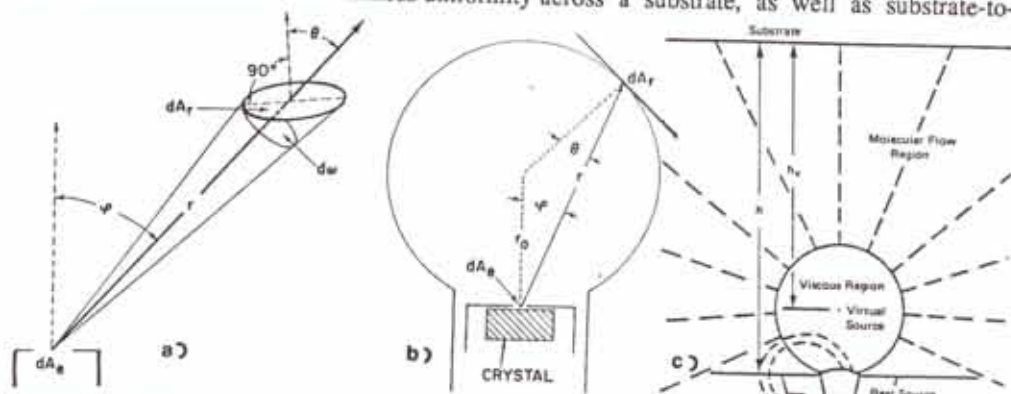


Fig. 40 (a) Surface element  $dA_r$  receiving deposit from a small-area source  $dA_s$ . (b) Evaporation from a small-area source onto a spherical receiving surface<sup>38</sup>. From L. Maissel and R. Glang, Eds., *Handbook of Thin Film Technology*, 1970. Reprinted with permission of McGraw-Hill Book Co. (c) Schematic diagram showing regions of viscous flow and molecular flow around an electron beam heated crucible. Courtesy of Temescal.

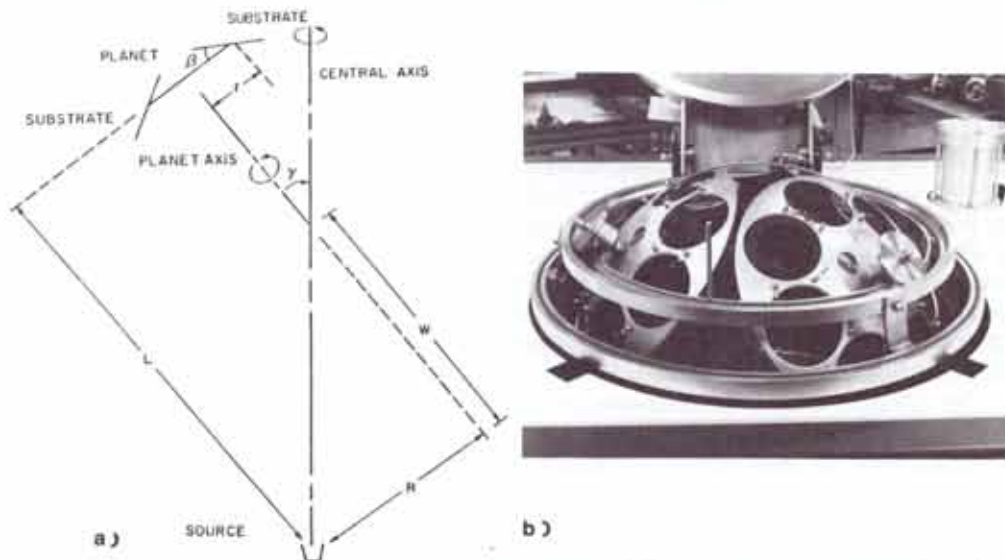


Fig. 41 (a) Schematic of planetary evaporator geometry<sup>48</sup>. Reprinted with permission of the American Physical Society. (b) Photograph of a planetary system. Courtesy of Temescal.

substrate. As a result, adequate control of film thickness and thickness uniformity is achievable.

The problem of maintaining adequate thickness as the film crosses steps, however, is not solved satisfactorily by the planetary<sup>48</sup>. That is, even when a planetary is used, thinning of the film and microcracks can occur, because of the shadowing effect of the step. Substrate heating (as discussed earlier), is one technique used to reduce the severity of this problem.

## Evaporation Methods

Evaporation is carried out under high-vacuum conditions. Typically the chamber is pumped down to  $\sim 5 \times 10^{-7}$  torr before the evaporation is initiated. At such pressures the mean free path,  $\lambda$ , is  $\sim 100$  m. As the source is heated, the pressure rises somewhat as contaminants are desorbed from its surface.

The least complex method of depositing thin films by evaporation is with *resistance-heated* sources. That is, a wire of low vapor pressure metal (e.g. W), is used to support small strips of the metal to be evaporated. The W-wire is then resistively-heated. The metal to be evaporated first melts and wets the heated filament, and evaporation ensues. Although the technique is simple, it has several drawbacks which make other evaporation techniques more useful for microelectronic applications, including: a) evaporation from the filament may contaminate the deposited film; b) refractory metals cannot be deposited because of their high melting points; and c) the small charges limit the ultimate film thickness. As a result, two other techniques have come to be widely adopted for performing evaporation depositions in microelectronic applications: 1) electron-beam evaporation; and 2) inductive-heating evaporation.

### Electron-Beam Evaporation

In electron beam evaporation, a stream of electrons is accelerated to high kinetic energy

(5-30 keV)<sup>40</sup>. The beam is directed at the material to be evaporated, and the kinetic energy is transformed to thermal energy upon impact. The electron stream can melt and evaporate any material, provided the beam can supply energy to the evaporant at an equal or greater rate than the rate at which heat is lost, as the material is held at high temperature. Electron beam *guns* (Fig. 42a and b) can be built to supply up to 1200 kW of highly concentrated electron beam power for evaporation applications. Very high film deposition rates can thereby be attained (e.g. 0.5  $\mu\text{m}/\text{min}$ ), as a result of the high power available.

The beam energy is concentrated on the surface of the target, and thus a molten region can be supported by a cooled structure. In fact, the target material itself provides a solid layer that separates the molten portion of the evaporant material from the wafer-cooled crucible. This eliminates the problem of reaction with, or dissolution of the crucible by the melt, and allows highly pure films to be deposited.

The self-accelerating, 270° beam guns have become the standard gun design. Earlier electron beam guns aimed the electron beam directly at the source, and hence the gun filaments would get coated and short circuited during the deposition cycle. In the 270° guns, a magnetic field simultaneously bends the beams through 270° and focuses them. The electron emission surface is hidden from the evaporating source, and the substrates are also protected from contamination by material evaporating from the heated filament. Movement of the beam (which allows the source to be scanned) is accomplished by electromagnetic deflection. This avoids the problem of nonuniform deposition that would be caused by the formation of a cavity in the molten source if the beam were stationary.

Two problems can arise from use of electron-beam evaporation: 1) At voltages >10 kV, the incident electron beam will cause Al to emit K-shell x-rays. These x-rays cause such damage as the creation of trapped charges in the gate oxides of MOS devices. The silicon devices interconnected by electron-beam Al must therefore be subjected to subsequent annealing to remove such damage, and as a result, restore device characteristics to their pre-metal deposition values; and 2) If excessive power is applied to the source, metal droplets that have been blown out of the source by the expanding metal vapor may be deposited on the substrates.

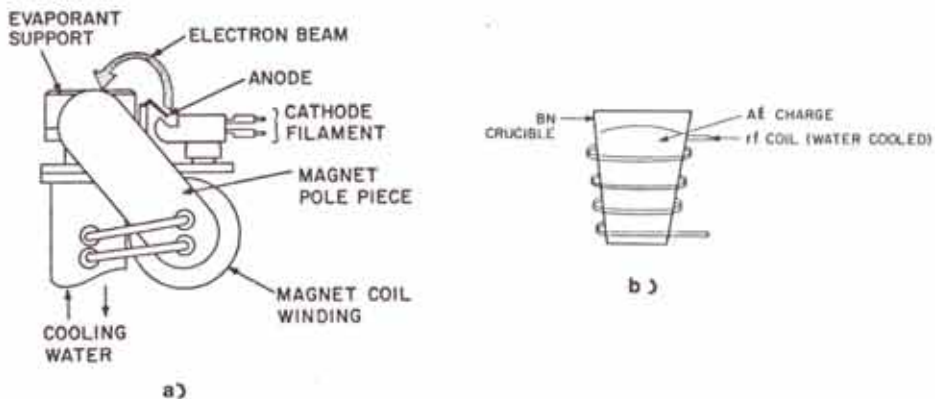


Fig. 42 (a) and (b) Bent beam electron gun. Courtesy of Temescal. (c) Inductively heated evaporation source. The molten Al charge is contained by the BN crucible.

### Inductive Heating Evaporation

High-rate evaporation deposition can also be accomplished by heating the source with rf energy. As shown in Fig. 42c, an rf induction heating coil surrounds a crucible containing the evaporation source. The crucible is commonly made of BN, because it is not attacked by molten Al, has excellent heat-shock resistance, and is an insulator that is easy to machine. The main advantage of inductive heating over electron-beam heating is that the wafers are not subject to ionizing radiation. Two of its disadvantages are: a) the mandatory use of a crucible that is in direct contact with the molten evaporant; and b) the increased complexity of rf equipment and process development.

### Evaporation Process Considerations

In addition to the information provided on evaporation, some topics related to practical processes need to be addressed including: a) evaporation of alloys; b) evaporation of multilayer films; c) effect of substrate temperature on aluminum film deposition; and d) use of shutters.

Evaporation of *alloys* is a complex process, since alloys consist of mixtures of elements that seldom have similar vapor pressures at a given temperature. In addition, *Raoult's Law* states that the vapor pressure of a solution is lower than that of a pure solvent by an amount proportional to the concentration of the solute. Alloy films are therefore evaporated using one of two techniques: a) evaporation from a *single source* composed of an alloy, but not necessarily containing the constituent elements in the same percentage ratio as in the deposited film; and b) simultaneous co-evaporation using *two electron guns and two sources*, with each source containing only one of the alloy constituents.

The *single-source method* is only practical if the vapor pressures are within a factor of 100 of each other at a given temperature. The composition of the film, however, is difficult to control, since as evaporation occurs, the compositions of both source and vapor change continuously. That is, the source becomes richer in the less volatile element. Alloy films of Al-0.5wt%Cu are typically evaporated using a single source of Al-2wt%Cu<sup>43</sup>.

The *dual-source* method offers the promise of better control, at the price of added system complexity. In addition, the uniformity of deposition across large substrates from two sources is reduced, and the relative power applied to the two sources must be well controlled to insure that the desired evaporation rates are maintained. By using the two-source method, however, it is even possible to co-deposit materials that form neither compounds nor solid solutions. Alloys of Al-Si are normally co-evaporated in two-source systems<sup>41,42</sup>. On the whole, however, it is significantly more difficult to deposit alloys with highly controlled compositions by either evaporation method than by sputter deposition.

*Multilayer films* can be deposited in a system containing several sources and a single electron-gun, or several guns can be aimed at multiple crucibles, to evaporate film layers in a planned sequence.

The variation of film thickness of Al films as they *cross steps* can be reduced in evaporation processes by applying heat to the substrates during deposition. For example, a significant improvement in Al film step coverage is observed as the wafer temperature is increased to 350°C during evaporation. The temperature increase is also seen to increase the grain size of the deposited film. As described in the sputtering discussion, substrate heating has the effect of creating greater surface mobility of the deposited material. Film atoms are thereby more likely to migrate toward regions which have received less material deposition. This enhances thickness

uniformity. Infrared lamps are commonly used to provide heat to the wafers.

*Shutters* are frequently employed in evaporation systems to prevent contaminants adsorbed on the source surface from being incorporated into the deposited films. That is, if the evaporation chamber and source are exposed to ambient conditions in the loading and unloading of wafers, the source surface may adsorb moisture, or form a native oxide layer. When the source is initially heated, such surface contaminants will vaporize (together with the source material). By interposing a shutter between the source and substrates (and postponing deposition by keeping the shutter closed until the source surface has been cleaned), the purity of the deposited film can remain uncompromised. Normally, the gas pressure rises upon initially heating the source and substrates, as a result of the contaminant desorption, and shutter opening is delayed until the chamber pressure returns to an acceptable level.

## METAL FILM THICKNESS MEASUREMENT and MONITORING

Metal thickness is usually monitored during evaporation, but is generally deposited without monitoring in sputter deposition. In both cases, the films are normally measured after deposition.

Post-deposition measurements of metal film thickness are most commonly performed either directly with a surface profiling device (known as a *stylus profilometer*), or indirectly by electrical measurement of sheet resistivity<sup>45</sup>. The basic aspects of sheet resistivity measurements are covered in Chap. 4, but it also should be mentioned at this point that the technique offers an important benefit for VLSI fabrication applications. That is, the probes can be stepped over a test wafer to provide contour maps of sheet resistance or thickness. This particular sheet resistance measuring method is discussed in more detail in Chap. 9, in the section dealing with

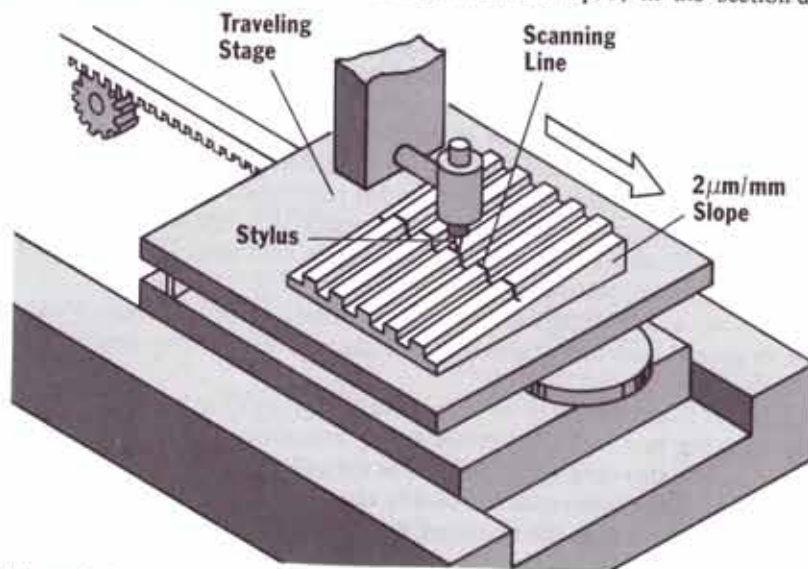


Fig. 43 Schematic drawing of a surface profilometer. Courtesy of Sloan Technology Corporation.

the monitoring of ion implant doses.

In the technique that uses the stylus profilometer, a step in the deposited film is first created, either by masking during deposition, or by a post-deposition etch process. Next, the profiling instrument draws a fine stylus along the surface containing the stepped film (Fig. 43). Whenever the stylus encounters a step, a signal variation (based on differential capacitance or inductance techniques), yields an indication of the step height. The information is displayed on a chart recorder or CRT. Two examples of commercially available instruments are the Sloan Dektak, and the Tencor Alpha-step. Films less than 1000Å thick can be measured with such instruments, but films much thinner than 1000Å are normally measured with sheet resistivity techniques. Vibration, surface roughness, and greater criticality of leveling the profilometer, all make such thin film measurements more difficult with the stylus-type instruments.

Periodic calibration of stylus profilometers is also required, using calibration standards traceable to the National Bureau of Standards. If the instrument is to be used to measure films whose thickness differ greatly from the calibration standard, a reference can be created by etching a step in thermally grown SiO<sub>2</sub>, and accurately measuring its height with an ellipsometer.

## REFERENCES

1. D. Pramanik and A.N. Saxena, "VLSI Metallization Using Aluminum and Its Alloys, pt I", *Solid State Tech.*, Jan. '83, p. 127, and pt. II, Mar. '83, p. 131.
2. F. Fischer and F. Nepl, "Sputtered Ti-Doped Al-Si for Enhanced Interconnect Reliability", *Proceedings IEEE Rel. Phys. Symposium*, 1984, p. 190.
3. D.S. Gardener, *et al.*, "Layered and Homogeneous Films for Al and Al-Si with Ti and W for Multilevel Interconnects", *IEEE Trans. on Electron Devices*, Feb. '85.
4. B. Chapman, *Glow Discharge Processes*, John Wiley & Sons, New York, 1980.
5. *The Book of Basics*, 3rd Ed., Materials Research Corp., no date, Orangeburg, N.Y.
6. W.D. Davis and T.A. VanderSlice, *Phys. Rev.* **131**, 219, (1963).
7. G.K. Wehner and G.S. Anderson, "The Nature of Physical Sputtering", in *Handbook of Thin Films*, Eds. L.I. Maissel and R. Glang, Chap. 3, McGraw-Hill, New York, 1970.
8. F. d'Heurle, L. Berenbaum, and R.A. Rosenberg, *Trans. Met. Soc. (AIME)* **242**, 502, (1968).
9. A.D. MacDonald and S.J. Tetenbaum, in *Gaseous Electronics*, Vol. I, Eds. M.N. Hirsh and H.J. Oskam, Academic Press, New York (1978).
10. H.R. Koenig and L.I. Maissel, *IBM J. Res. Develop.*, **14**, 168 (1970).
11. W.H. Class, "Focest Cathode DC Magnetron Deposition of Conductor Metallization", *Solid State Technology*, June, 1983, p. 103.
12. J.L. Vossen and J.J. Cuomo, "Glow Discharge Sputter Deposition", in *Thin Film Processes*, Eds. J.L. Vossen and W. Kern, Academic Press, New York, 1978, Chap. II-1, p. 11-73.
13. J.A. Thornton and A.S. Penfold, "Cylindrical Magnetron Sputtering", in *Thin Film Processes*, Eds. J.L. Vossen and W. Kern, Academic Press, New York, 1978, p. 75.
14. G.K. Wehner and G.S. Anderson, "The Nature of Physical Sputtering", in L.J. Maissel and R. Glang, Eds., *Handbook of Thin Film Technology*, McGraw-Hill, New York, 1970, Chap. 3.
15. L. Maissel, "Application of Sputtering to Deposition of Films", in L. Maissel and R. Glang, Eds., *Handbook of Thin Film Technology*, McGraw-Hill, New York, 1970, Chap. 4.
16. H.F. Winters and E. Kay, *J. Appl. Phys.*, **38**, 3928 (1967).
17. J.L. Vossen and J.J. O'Neil Jr., *RCA Review* **29**, 566 (1968).
18. J.L. Vossen and J.J. O'Neil Jr., *RCA Review* **31**, 276 (1970).